*Review*

# Application of PEDOT:PSS and Its Composites in Electrochemical and Electronic Chemosensors

Nan Gao [1], Jiarui Yu [1], Qingyun Tian [2], Jiangfan Shi [3], Miao Zhang [2], Shuai Chen [1,4,*] and Ling Zang [3,*]

[1] Flexible Electronics Innovation Institute, School of Pharmacy, Jiangxi Science & Technology Normal University, Nanchang 330013, China; gaonan2019@163.com (N.G.); yujiarui411@163.com (J.Y.)
[2] School of Environmental Science and Engineering, Shaanxi University of Science and Technology, Xi'an 710021, China; tianqingyun2017@163.com (Q.T.); miaozhang1209@163.com (M.Z.)
[3] Department of Materials Science and Engineering, Nano Institute of Utah, University of Utah, Salt Lake City, UT 84112, USA; jfan_shi@163.com
[4] Jiangxi Engineering Laboratory of Waterborne Coatings, Nanchang 330013, China
[*] Correspondence: shuaichen@jxstnu.edu.cn (S.C.); lzang@eng.utah.edu (L.Z.); Tel.: +1-801-587-1551 (L.Z.); Fax: +1-801-581-4816 (L.Z.)

**Abstract:** Poly(3,4-ethylenedioxythiophene):polystyrene sulfonate (PEDOT:PSS) is a highly important and attractive conducting polymer as well as commercially available in organic electronics, including electrochemical and electronic chemosensors, due to its unique features such as excellent solution-fabrication capability and miscibility, high and controllable conductivity, excellent chemical and electrochemical stability, good optical transparency and biocompatibility. In this review, we present a comprehensive overview of the recent research progress of PEDOT:PSS and its composites, and the application in electrochemical and electronic sensors for detecting liquid-phase or gaseous chemical analytes, including inorganic or organic ions, pH, humidity, hydrogen peroxide ($H_2O_2$), ammonia ($NH_3$), CO, $CO_2$, $NO_2$, and organic solvent vapors like methanol, acetone, etc. We will discuss in detail the structural, architectural and morphological optimization of PEDOT:PSS and its composites with other additives, as well as the fabrication technology of diverse sensor systems in response to a wide range of analytes in varying environments. At the end of the review will be given a perspective summary covering both the key challenges and potential solutions in the future research of PEDOT:PSS-based chemosensors, especially those in a flexible or wearable format.

**Keywords:** PEDOT:PSS; chemosensor; electrochemistry; chemoresistive; organic electronics

## 1. Introduction

It remains imperative to develop chemosensor techniques for environmental, health and safety monitoring [1,2]. With the technical advancement in instrumentation, microelectronics and computers, it becomes more feasible nowadays to design and construct chemosensors utilizing most of the known chemical, physical and biological properties or features of sensor materials. Chemosensors may be classified into different types according to the sensor operating principle. Typical types of chemosensors include optical [3] (based on colorimetric or fluorescence change), electrical [4] (based on measurement of resistance, capacitance, impedance or other electrical signal), IR spectrometry, mass spectrometry, chromatography, surface acoustic wave, and others. Among all these types of sensors, chemosensors based on electrical signal modulation are much more straightforward and facile for device design, signal transduction and system integration, which combined can be made to be portable and small in size, thus suited for real-time onsite operation. Electrochemical [5] and electronic signals [6] are mostly used in electrical mode chemosensors. Upon exposure to the chemical analytes, an electrochemical sensor can transform the amperometric, potentiometric, or voltammetric effect of the analyte–electrode interactions (mostly in liquid solutions) into a measurable signal that in turn can identify and quantize

the presence of different analytes [4]. In comparison, an electronic chemosensor usually outputs a signal directly arising from the change of electrical properties (resistive, conductivity, etc.) of the sensor material caused by the surface charge-transfer interaction with chemical analytes (mostly in the gas phase).

The overall performance of chemosensors is determined by several factors such as chemical and physical properties of sensing material, device geometry, and signal transduction. Improvement of the sensor performance demands a synergistic optimization of the above-mentioned factors. In terms of sensing materials, diverse conductive materials such as conducting polymers, polymer/carbon composites, graphene, and metal or semiconductor nanocrystals show great promise [7]. Especially, conducting polymers such as poly(3,4-ethylenedioxythiophene) (PEDOT) [8], polypyrrole (PPy) [9] and polyaniline (PANI) [10] are among the highest attractive sensing materials owing to their intriguing features such as their all-organic nature with good designability, intrinsic electrical conductivity, high signal transduction, dimensional durability, mechanical flexibility, and chemical stability. The synthesis of the polymers, usually via convenient chemical or electrochemical polymerization methods, are simple and cost effective. The polymers thus synthesized can retain their electrical conductivity and chemical/physical stability when used in chemosensors. Such durability is crucial for chemosensors, for which the sensing repeatability is one of the most important factors affecting the real application of sensor devices.

Among the conducting polymers used for chemosensors, PEDOT exhibits a relatively high stability and adjustable conductivity ($10^{-3}$–$10^3$ S cm$^{-1}$) compared to PPy and PANI. The linear, rigid molecular conformation of PEDOT facilitates its charge transport [11]. To be suited for use in chemoresistive sensors, the conductivity of polymers must be at an appropriate level and, more importantly, adjustable. Indeed, if the conductivity is too low or too high, the sensor performance will be limited by the low signal-to-noise ratio [12]. PEDOT by itself is typically insoluble in water or common organic solvents [13]. However, if it is synthesized in the presence of poly(4-styrenesulfonate) (PSS), an stable aqueous dispersion containing both polymers (PEDOT:PSS) (Figure 1b) can be obtained, which is normally of a dark-blue color [14]. As a commercially available and ready-to-use waterborne dispersion, PEDOT:PSS remains attractive for development as organic electronics (including thermoelectric conversion [15], photovoltaic devices [16], supercapacitors [17] and sensors [18], etc.) because of its excellent solution-fabrication capability and miscibility into functionally films (usually by drop-casting [19], spin-coating [20], and spray-coating [21]) exhibiting a high and controllable conductivity, a high work function, excellent chemical and electrochemical stability, good optical transparency, good biocompatibility, and so on [22]. Since year 2000 when the three discoverers of conducting polymers won the Nobel Prize in Chemistry, PEDOT:PSS and its hybrid composites with metal/metal oxide nanoparticles, insulating polymers, carbon materials and others have been extensively studied and applied widely in organic electronics including electrochemical and/or electronic chemosensors as covered in this review. These research activities have produced thousands of peer-reviewed papers and patents.

In the last decade, some excellent reviews have been published on the related topics of electrical sensors based on various conducting polymers. For example, Liao et al. [23] reviewed the development of organic electrochemical transistor (OECT)-based sensors by focusing on the functionalization of PEDOT:PSS films as channel materials. Rahimzadeh et al. [13] reviewed the recent advancement in PEDOT-based electrochemical biosensors. Various PEDOT composites blended with nanomaterials such as carbon nanomaterials and metal/metal oxide nanoparticles, and the applications in electrochemical sensors were described by Kaur et al. [18] However, there still lacks a special and comprehensive review of electrochemical and electronic chemosensors based on PEDOT:PSS and its composites.

In this review, we will focus on the recent research progress of PEDOT:PSS and its composites, and the application in electrochemical and electronic sensors for detecting liquid-phase or gaseous chemical analytes, including inorganic or organic ions, pH, humidity, hydrogen peroxide ($H_2O_2$), ammonia ($NH_3$), CO, $CO_2$, $NO_2$, and organic solvent

vapors like methanol, acetone, etc. We will discuss in detail the structural, architectural and morphological optimization of PEDOT:PSS and its composites with other additives, as well as the fabrication technology of diverse sensor systems in response to a wide range of analytes in varying environments. It is expected that this review will not only provide a deep, comprehensive understanding of the structure, architecture and composite design rules, chemical stimuli response mechanisms, and sensing processes of PEDOT:PSS-based electrochemical/electronic chemosensors, but also help extend the research of PEDOT:PSS-based composites into other emerging areas, especially flexible, stretchable, and wearable electronics, for which chemosensors play crucial roles in the development of multimodal sensors and related system integration.

## 2. PEDOT:PSS-Based Electrochemical Chemosensors

A typical electrochemical sensor has been considered as electrochemical cells containing three or two electrodes (Figure 1a) immersed in an electrolyte solution. A characteristic three-electrode system contains a reference, counter, and working electrode (sensing electrode). The working electrode has a chemically stable solid conductive substance (conventionally gold, carbon, and platinum), and the reference electrode generally contains the silver wire coated with a layer of silver chloride (Ag/AgCl) to provide a fixed stable potential to other electrodes, and a platinum wire is usually employed as the counter electrode (not necessary in a two-electrode system) to the working electrode. The electrochemical procedures can usually be classified into three key categories concerning different modes of measurement: current (voltammetry, amperometry), potential difference (potentiometry), and impedance (electrochemical impedance spectroscopy) [11]. The common current mode-based sensors are to measure the current under the potential of a working electrode against a reference electrode. This electrical current results from the electrolysis of chemical analytes (e.g., molecules, ions) through either electrochemical oxidation or reduction at the working electrode surface. This procedure depends on the mass transport rate of the analytes to the electrode, as well as the rate of electron transfer at the electrode surface. In addition to the conventional electrochemical systems, OECT (Figure 1b) is another sensor architecture commonly used in chemical and biological detection. In a regular OECT configuration, the gate is immersed in an electrolyte and the active material channel is in direct contact with an electrolyte and with the source and drain [24]. The important sensing interfaces for analyte monitoring are the gate electrode surface and channel surface. Any chemical reaction occurring on these two surfaces may induce a change in interfacial potential, and result in a change in channel current, which in turn can be used as a sensor response signal [23].

It is important to note that for the development of electrochemical chemosensors to determinate different analytes, the working electrodes have often been modified with appropriate substances to achieve the desired performance such as improved selectivity, sensitivity and stability. PEDOT:PSS has not only been employed as a common material for working electrodes, but has also been proven compatible and processible with metal or carbon materials for surface modification. Besides, good biocompatibility of PEDOT:PSS makes it an ideal material for bioelectronic applications. PEDOT:PSS is an excellent matrix for functionalization with various biological components such as antibodies [25], enzymes [26], and peptides [27] to be developed as electrochemical biosensors. There are several reviews [2,5,28] focused on such electrochemical biosensors integrated with conducting polymers including PEDOT:PSS for monitoring the biological targets such as DNA, proteins [27], glucose [29], and other biomarkers. In this section, we just give a brief summary about this aspect of research, while the main attention will be laid on the issues and improvements of electrochemical chemosensors towards biological and environmental analytes such as $H_2O_2$, pH, $NH_4^+$, some inorganic ions and organic compounds, etc. (Table 1).
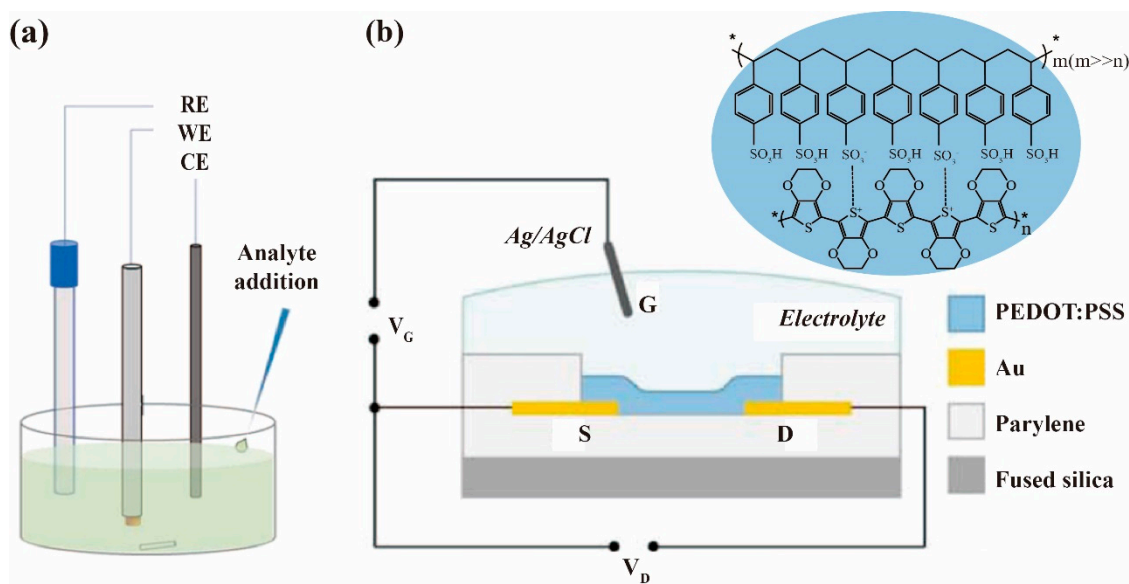
**Figure 1.** Schematic architectures of electrochemical chemosensors based on PEDOT:PSS: (**a**) three- or two-electrode electrochemical system (RE = reference electrode, WE = working electrode, CE = counter electrode) [30]; (**b**) OECT device [31].

### 2.1. $H_2O_2$ Detection

Hydrogen peroxide ($H_2O_2$) has been widely used in industry as it plays crucial roles in chemical, pharmaceutical, and food manufacturing [32]. $H_2O_2$ is also an important component or synthetic precursor for some improvised explosives. Moreover, $H_2O_2$ is a key marker in biological processes as it is involved in signaling paths such as cellular growth, senescence and apoptosis, wherein it can be generated through different stimuli. Detection of $H_2O_2$ can help probe the biomolecules in different fluids as $H_2O_2$ is often a byproduct of many biochemical reactions involving oxidase enzymes such as glucose, cholesterol and lactate oxidase, etc. For these reasons, the development of chemosensors for trace level detection of $H_2O_2$ has remained the focus of chemosensor research, for which most of the sensors reported are based on electrochemical system owing to the electroactive nature of $H_2O_2$. In this section, we focus on the direct detection of $H_2O_2$, and exclude the indirect detection of $H_2O_2$ as a byproduct of a redox reaction.

As shown in Table 1, most of the electrochemical sensors developed for $H_2O_2$ are amperometric types and used glassy carbon electrode (GCE) or a screen-printed electrode (SPE) as the working electrode substrate. GCE has the advantages of wide commercial availability, a low background current, and easy surface modification, while SPE is small in volume and easy to be integrated in a sensor system for miniaturization.

The main architecture of components of a typical working electrode for electrochemical detection of $H_2O_2$ is shown in Figure 2. The electrochemistry technique based on a simple and low-cost enzyme electrode has been extensively employed for accurate determination of $H_2O_2$ due to the intrinsic selectivity and sensitivity of enzymatic reactions [33,34]. The most frequently used enzyme to decompose $H_2O_2$ is horseradish peroxidase (HRP), which catalyzes the oxidation of a substrate using $H_2O_2$ as the oxidizing agent, allowing for direct electron transfer through the electrode. In this situation, PEDOT:PSS was coated on the electrode to immobilize HRP because of its good conductivity and biocompatibility, providing an ideal microenvironment for keeping biological activity while facilitating the direct electron transfer between the enzyme's active sites and the electrode. After the surface modification of the electrode and immobilization of the enzyme, a Nafion film is usually coated to prevent the modification layer from falling off because PEDOT:PSS is prone to swell and fall off from the substrate in an aqueous solution.
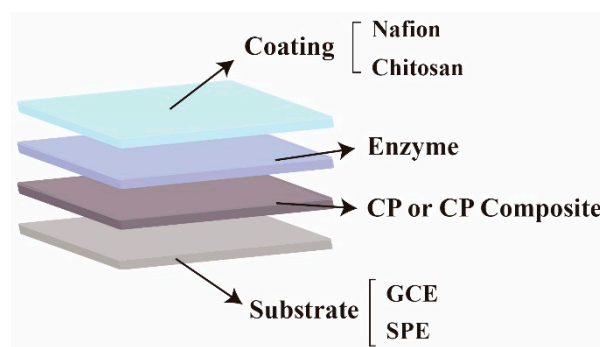
**Figure 2.** Component architecture of the working electrode based on PEDOT:PSS or its composite for electrochemical detection of $H_2O_2$.

As an example of success, Zhang et al. [33] fabricated a hybrid composite of PEDOT:PSS and chitosan micelles and coated it on the surface of GCE, followed by immobilization with HRP. The presence of PEDOT:PSS was found to be capable of enhancing the interfacial electron transfer between HRP and the electrode. The sensor thus fabricated showed a very low detection limit (LDL) of 0.03 nM and a dynamic linear range between 0.1 nM and 10 nM for detection of $H_2O_2$. The wide detection range was attributed to the large surface area of the hybrid film of PEDOT:PSS, which in turn facilitates the immobilization of HRP. The large surface area would also facilitate the signal transduction from the enzyme to the electrode. The similar advantage of a large surface area of electrode for improving the sensor performance was also evidenced in a sensor involving PEDOT:PSS hydrogel, which was also conducive to a high loading of enzymes like HRP [34].

In recent years, gold nanoparticles (AuNPs) and silver nanoparticles (AgNPs) have been widely used in the fabrication of electrochemical biosensors because of their unique properties such as high biocompatibility, good conductivity, high catalytic activity, and size-dependent properties. Compared to the pristine PEDOT:PSS, the composites with an encapsulation of the metal nanoparticles could further enhance the electron exchange and realize the direct electrochemical redox reactions of enzymes since metal nanoparticles may act as electron relays in the PEDOT:PSS film. As evidenced in many studies, the GCEs modified with HRP/PEDOT:PSS/AuNPs [35] and HRP/PEDOT:PSS/AgNPs [36] showed excellent electrocatalytic ability and were thus sensitive to detection for $H_2O_2$ with a wide linear range of 0.2~380 μM and 0.05~20 μM, respectively. More sophisticated, a ternary composite [37] with PEDOT:PSS, AuNPs and reduced-graphene oxide (rGO) was assembled with HRP on a screen-printed gold electrode (SPGE) for amperometric detection of $H_2O_2$. This composite sensor exhibited a high sensitivity of up to 677 A $mM^{-1}$ $cm^{-2}$, with a wide linear range from 5 to 400 μM and LDL of 0.08 μM. The enhanced sensing performance could be ascribed to the intimate contact of AuNPs onto the rough surface of the PEDOT:PSS-rGO nanocomposite, which has a high electrical conductivity and a large surface area, allowing for the growth and support of nanoparticles while still maintaining the high electrical conductivity.

While PEDOT:PSS and other materials have been commonly used to immobilize enzymes on an electrode for retaining the enzymatic biologic activity and electrically connecting the enzyme with the electrode surface, the research of PEDOT:PSS-based electrochemical sensors for $H_2O_2$ has also been extended from use of enzymes to enzymeless active composites such as Meldola Blue (MDB) and Prussian Blue (PB). This alternative approach aims to overcome the technical limitations of enzymes like poor stability and the complexity of the immobilization process involving enzymes. Siao et al. [38] reported an enzymeless electrochemical sensor for $H_2O_2$, which was fabricated with PEDOT:PSS and Meldola Blue (MDB) on a GCE. The sensor thus fabricated could electrocatalytically reduce $H_2O_2$ with a low overpotential and showed a linear response in the concentration range of 5 to 120 μM with a LDL of 0.1 μM and a sensitivity of 353.9 μAmM$^{-1}$ $cm^{-2}$.

Although electrochemical sensors are usually suitable for detection of analytes in solutions, there exists a potential to adapt the sensor for gas phase chemical detection by combining the sensor system with an air extraction system that can concentrate airborne analytes into solution to be ready for electrochemical detection. Recently, Chen et al. [19] prepared a new composite consisting of PEDOT:PSS, PB, ethylene glycol (EG), and divinyl sulfone (DVS). After drop-casting it onto a SPGE, the sensor showed a good linear response between 0.1 μM to 25.6 μM with a sensitivity of $-0.95$ A M$^{-1}$ cm$^{-2}$ and LDL of 0.22 μM for solution phase detection. When combing the sensor with an exhaled breath condensate (EBC) device, it became capable of directing detection of $H_2O_2$ in human breath, which may provide a new way for noninvasive diagnosis or screenings of diseases (e.g., cancers) as $H_2O_2$ has been identified as one of the common breath biomarkers for humans.

### 2.2. pH Detection

pH is an extremely important parameter in biological processes and related chemical reactions. Detection of pH changes can provide diagnostic information about health and medical status. In particular, pH variations in human sweat have been correlated to blood glucose levels [39] and the pH of a wound exudate is indicative of the progression of the wound-healing process and the presence of bacterial colonies [40]. Real-time analysis of such biofluids can be achieved by means of portable and wearable sensing devices integrated into clothing, bandages or other everyday accessories, which imposes a great technical challenge to the traditional chemical sensors. While much effort has been put into combining flexible substrates with traditional rigid sensing materials to fabricate pH sensors with a good performance, the flexibility of PEDOT:PSS film and its biocompatibility for wearable bioelectronics are beyond the reach of these technologies. Within the PEDOT:PSS composite, the PEDOT chains are uniformly distributed along the PSS polymer chains under slightly acidic conditions. Such an optimized distribution of PEDOT chains within the colloidal PEDOT:PSS system ensures the formation of a continuous electrical connection between PEDOT segments. When the pH shifts from acidic to basic, the homogeneous distribution of PEDOT along the PSS polymer chains is interrupted by the negatively charged hydroxyl groups. Under more basic conditions, the PEDOT short chains are neutralized by the hydroxyl groups, forming a new hydrophobic phase which is covered by the long chains of PSS [41] (Figure 3a). As a result, conductivity of the polymer film declined significantly. However, swelling of the hydrophilic PSS in PEDOT:PSS could affect the resistance of the electrode, leading to poor pH sensitivity in electrochemical sensors. In general, electrochemical sensing of pH relies on the potentiometric measurement of an active working electrode with respect to the reference electrode.

The conductivity of PEDOT:PSS used in the electrochemical sensors can be improved by various methods [42] in order to overcome the above-mentioned technical limitations. The PEDOT:PSS composite is often fabricated with other pH-sensitive materials acting as a charge transfer layer of work electrode. PANI, for example, has low conductivity, but its various oxidation states are pH-dependent, making it suitable for pH sensing. Smith et al. [40] deposited the dispersions of PEDOT:PSS and multiwalled carbon nanotubes (MWCNTs) on cotton (Figure 3b,c) by a dipping method, followed by electrochemical deposition of PANI to fabricate a fibril material to function as the working electrode. The fiber electrode showed a rapid response ($-61 \pm 2$ mV pH$^{-1}$) over a wide pH range (2–12) and a high selectivity in the presence of varying interfering ions ($NH_4^+$, $Mg^{2+}$, $Ca^{2+}$, $K^+$ and $Na^+$). The PANI/PEDOT:PSS-MWCNTs-cotton fibril composite showed intermediate values of ultimate tensile strengths ($130 \pm 25$ MPa, $10 \pm 2\%$ strain at break) whilst maintaining sufficient flexibility. The fibril materials have an obvious ability to inhibit the growth of bacteria and has biocompatibility with skin cells. This highlights the potential to develop these fibril materials as pH-sensing fabrics for wound monitoring. Smith et al. [43] also directly prepared PEDOT:PSS fibers (Figure 3d) by wet spinning and then electrodeposited PANI onto them for pH detection. The pristine PEDOT:PSS fibers were treated with dimethyl sulfoxide (DMSO) and their diameters were controlled to obtain

a high conductivity ($802 \pm 122$ S cm$^{-1}$). The thicker fibers have a higher PSS-to-PEDOT ratio, which leads to more water being absorbed by the hydrophilic PSS, resulting in more swelling during pH analysis. This would affect the resistance of the electrode and thus the potential and slope of voltage vs. pH (Figure 3e). The best pH response and lowest swelling was achieved by the thin fiber prepared from DMSO treatment, which gave a response of $-56 \pm 7$ mV pH$^{-1}$.
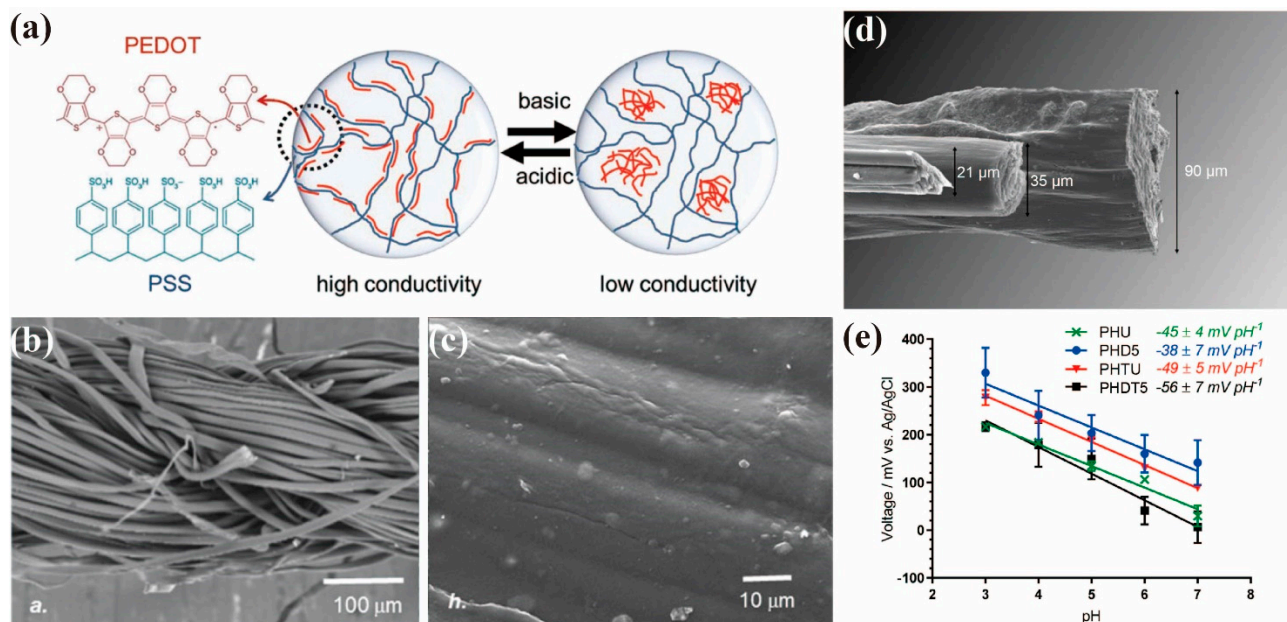


**Figure 3.** (**a**) Schematic illustration of the impact of pH on molecular structure of PEDOT:PSS [41]; SEM images of (**b**) uncoated cotton and (**c**) PEDOT:PSS-MWCNTs-cotton [40]; (**d**) SEM image comparing three fiber type; (**e**) Potentiometric (open circuit) response of PEDOT:PSS wet-spun fibers coated with PANI. (PHU: 90 μm PEDOT:PSS fibers without DMSO treatment; PHD5: 90 μm PEDOT:PSS fibers with 5 min DMSO treatment; PHTU: 20 μm PEDOT:PSS fibers without DMSO treatment; PHDT5: 20 μm PEDOT:PSS fibers with 5 min DMSO treatment) [43].

### 2.3. Ion Detection

When PEDOT:PSS is introduced into an ion sensor, it acts as an ion-to-electron transducer layer to decrease the impedance and promote the charge transfer within the sensor, which significantly improves the potentiometric stability and detection performance. The selectivity of such an ion sensor comes from the use of an ion-selective membrane (ISM). ISM allows for only specific ions to transport from the solution to the conductive layer, whereas it blocks the transport of other interfering ions, thus enabling selective detection of a variety of cations and anions such as Na$^+$, K$^+$ [44], Ca$^{2+}$, NH$_4^+$ [45], Cu$^{2+}$ [46], Mg$^{2+}$, Cl$^-$ [47], etc.

For many years, direct potentiometry and ion-selective electrodes have been useful tools for determining ion concentrations in human body fluids and other areas in medical analyses. Urbanowicz et al. [47] fabricated a two-layer surface coating on the gold electrode: electrically synthesized PEDOT:PSS forming an intermediate layer and ISM, to monitor Na$^+$, K$^+$, Ca$^{2+}$, Mg$^{2+}$ and Cl$^-$ in human saliva (Figure 4a). The sensor consisted of a reference electrode and an ion selective electrode, showing a wide linear range and sensitivity (Table 1) assuring its applicability in biomedical fields.

PEDOT:PSS is characterized by high stability, high ionic mobility and a high charge transfer rate, as well as good adhesion to the membrane material and electrode substrate. The most common ways to deposit PEDOT:PSS onto the electron conductive substrate are via drop-casting, spin-coating, or inkjet printing, etc. However, as reported in many publications, the films of the same conducting polymer fabricated with different deposition methods may show different characteristics [48]. These factors affect the reproducibility

of electrical potentials, which are critical characteristics for the mass production of ion-selective electrodes. In this regard, Wang et al. [49] studied a $Ca^{2+}$ sensor based on a screen-printing technique, that is, PEDOT:PSS was screen-printed on carbon paste electrodes as internal solid contacts for both ion-selective and reference electrodes. The screen-printing method provides a cost-effective and reproducible way of mass-manufacturing portable ion sensors.

Recently, Coppedè et al. [44] fabricated a textile OECT device (Figure 4b) by soaking an acrylic textile thread with PEDOT:PSS. The selectivity was improved by directly functionalizing the textile device with ISM. Membrane selectivity was tested by comparing the transistor response with interfering ions, proving successfully the selective response to $Na^+$, $K^+$, $Ca^{2+}$. This direct functionalization of textile fibers as an active channel may find wide application in the wearable devices for analyzing liquid samples, such as sweat, enabling real-time monitoring and screening of health.
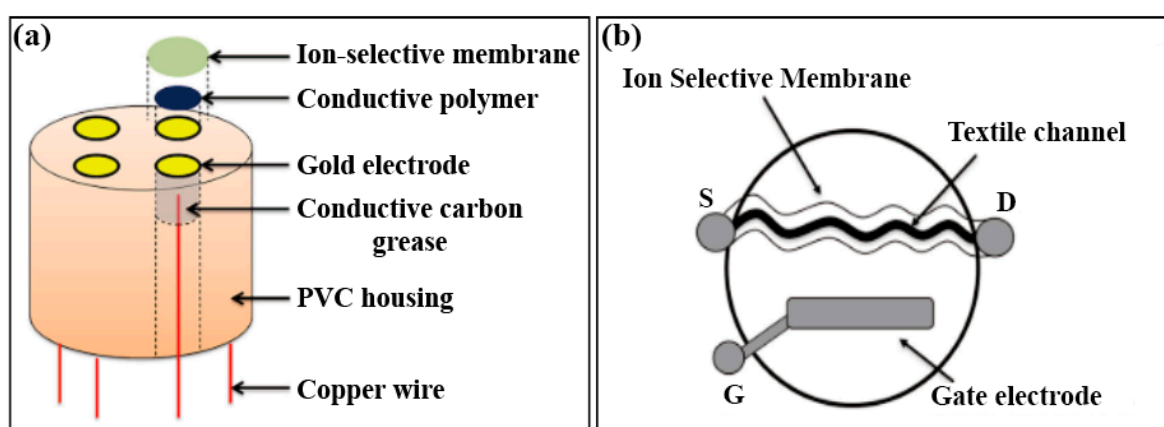


**Figure 4.** (**a**) Schematic illustration showing the architecture of working electrode for multiple ion sensing [47]; (**b**) sketch of a OECT type sensor fabricated with textile channel coated with ion selective membrane [44].

*2.4. Other Analyte Detection*

As described above, in electrochemical sensors, the sensing signal comes from the redox reaction of the analyte on the electrode surface. PEDOT:PSS is used to modify the bare electrode to improve the detection sensitivity due to its excellent electrochemical and environmental stability, good biocompatibility, superior film-forming properties, and fine tuning of their physicochemical properties [50,51]. In addition, researchers have often combined PEDOT:PSS with different nanoscale catalytic materials (mainly carbon materials [52–55] and metal/metal oxide nanoparticles [56–59]) to form composites in order to promote rapid electron transfer. Such an approach has great potential for application in the construction of electrochemical sensors for various biological and environmental detections [18].

The incorporation of different nanostructures into PEDOT:PSS generally improves the interaction and the electrocatalytic activity with the analyte in a synergistic way, which leads to an amplified signal output. As shown in Figure 5a, carbon black (CB), graphene oxide (GO), copper nanoparticles (CuNPs) and PEDOT:PSS can be mixed and used for surface modification of the GCE electrode [57]. The cyclic voltammograms of the GCE electrode before and after modification with a PEDOT-PSS film containing GO, CB-GO or CuNPs/CB-GO was shown in Figure 5b. It is clear that the peak current was relatively increased after each step of modification, indicating that the electroactive surface area of GCE increased after every modification. And the quinary mixtures of isoproterenol, acetaminophen, folic acid, propranolol and caffeine was determined by square-wave voltammetry (Figure 5c), resulting the linear ranges and LDL of micromolar concentration levels, as shown in Table 1.
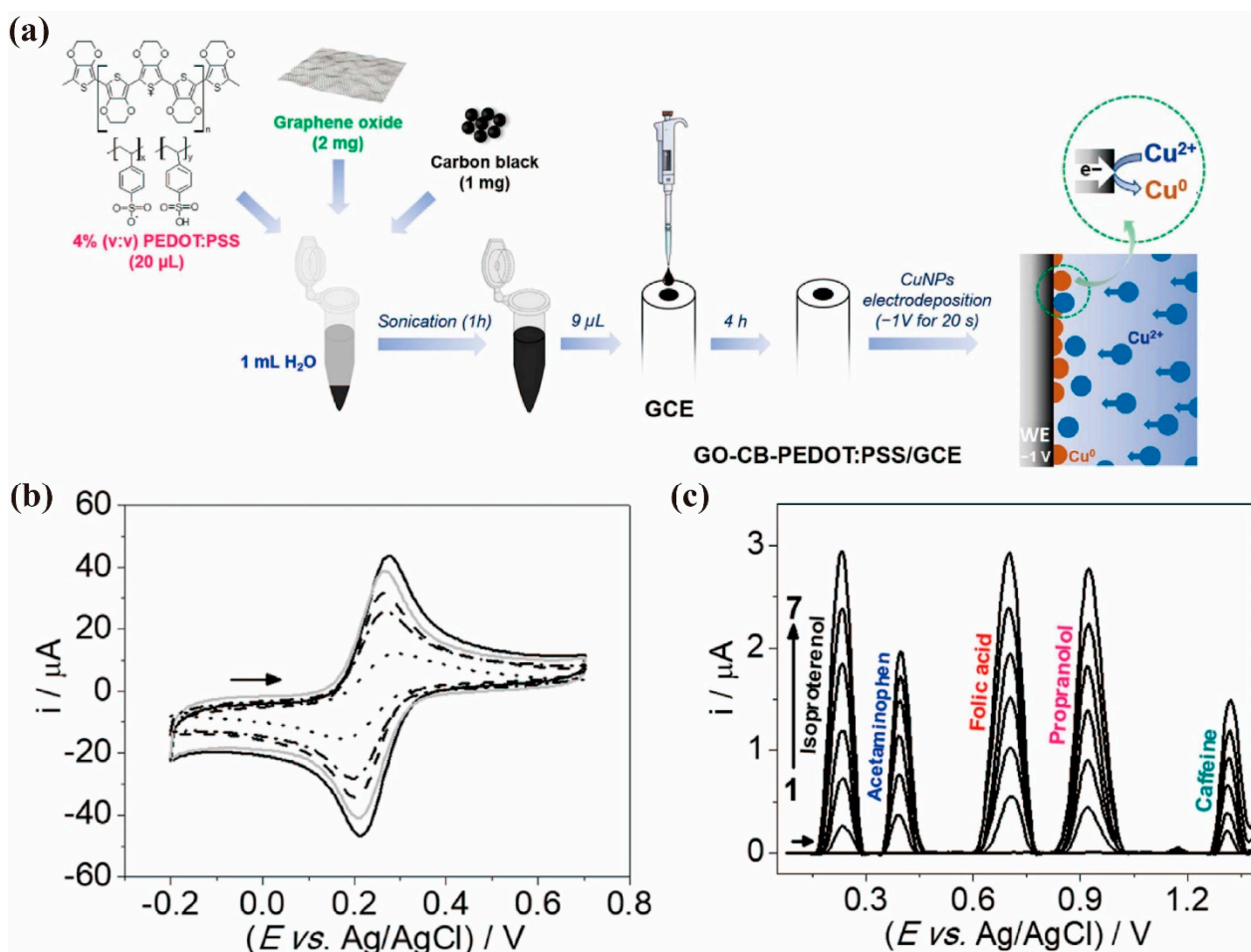
**Figure 5.** (**a**) Scheme of the fabrication of CuNPs/CB-GO-PEDOT:PSS/GCE electrode; (**b**) Cyclic voltammograms obtained by using unmodified GCE ( . . . ..), PEDOT:PSS/GCE (— · —), GO-PEDOT:PSS/GCE (— —), CB-GO-PEDOT:PSS/GCE (——) and CuNPs-CB-GO-PEDOT:PSS/GCE (——); (**c**) Square-wave voltammograms of the response to diverse analytes obtained on a CuNPs/CB-GO-PEDOT:PSS/GCE [57].

In addition, various other methods have been proven to be quite useful for fabrication of low-resistance PEDOT:PSS films for electrochemical analyte detection [49,59,60]. For example, our group [60] prepared PEDOT:PSS films with enhanced conductivity by DMSO second-doping, which can be directly used as flexible electrodes for detection of *p*-butylhydroquinone (TBHQ), which gave a LDL of 0.15 µM. However, the poor water resistance and weather stability of the PEDOT:PSS film would limit the widespread application in electrochemical analysis. To solve this problem, Zhang et al. [61] introduced carboxymethyl cellulose (CMC) into PEDOT:PSS, which demonstrated a significant improvement of the flexibility, adhesion and long-term electrode stability in water, as well as the electrocatalytic ability for maleic hydrazide (MH), salicylic acid (SA), and sunset yellow. In their subsequent work [62], a carbon nanotube with a large rough surface area was added to the composite of PEDOT:PSS and CMC to improve the electrochemical sensing performance of PEDOT:PSS composites. The fabricated PEDOT:PSS-CMC-SWCNT/GCE exhibited enhanced electron transfer and a synergistic electrocatalytic ability towards maleic hydrazide, and displayed excellent sensing performance with a wide linear range (0.8 to 51 µM), a low LDL (0.1 µM) and good sensing stability.

**Table 1.** Comparison of PEDOT:PSS-based electrochemical chemosensors for different analytes.

| Working Electrode | Analyte | Model | LDL | Sensitivity | Linear Range | Ref. |
|---|---|---|---|---|---|---|
| PEDOT:PSS-PB-EG-DVS/SPGE | $H_2O_2$ | Amperometry | 219 nM | $-0.95$ A $M^{-1}$ $cm^{-2}$ | 0.1–25.6 µM | [19] |
| Nafion/HRP/PEDOT:PSS-CS micelle/GCE | $H_2O_2$ | Amperometry | 0.03 nM | - | 0.1 nM–10 nM | [33] |
| Nafion/HRP/PEDOT:PSS hydrogel/GCE | $H_2O_2$ | Amperometry | 0.94 µM / 0.045 mM | 155 µA $mM^{-1}$ / 3.5 µA $mM^{-1}$ | 0.0088–0.15 mM / 0.4–10 mM | [34] |
| HRP-PEDOT:PSS-AuNPs/GCE | $H_2O_2$ | Amperometry | 0.1 µM | - | 0.2–380 µM | [35] |
| Nafion/HRP/AgNPs/PEDOT:PSS-Nafion/GCE | $H_2O_2$ | Amperometry | 0.02 µM | - | 0.05–20 µM | [36] |
| HRP/PEDOT:PSS-rGO-AuNPs/SPGE | $H_2O_2$ | Amperometry | 0.08 µM | 677 µA $mM^{-1}$ $cm^{-2}$ | 0.5–400 µM | [37] |
| PEDOT:PSS-MDB/GCE | $H_2O_2$ | Amperometry | 0.1 µM | 353.9 mA $mM^{-1}$ $cm^{-2}$ | 5–120 µM | [38] |
| PANI/PEDOT:PSS/G | pH | Potentiometry | - | 75.06 mV $pH^{-1}$ | 4–7 | [39] |
| PANI/PEDOT:PSS-MWCNTs-cotton | pH | Potentiometry | - | $-61 \pm 2$ mV $pH^{-1}$ | 2–12 | [40] |
| PANI/PEDOT:PSS fiber | pH | Potentiometry | - | $-56 \pm 7$ mV $pH^{-1}$ | 3–7 | [43] |
| $K^+$ ISM/PEDOT:PSS-acrylic textile | $K^+$ | OECT | - | 3.49 $M^{-1}$ | 0.01–1000 mM | [44] |
| $NH^{4+}$ and $Ca^{2+}$ ISM/PEDOT:PSS | $NH^{4+}$ / $Ca^{2+}$ | OECT | - | - | 10–1000 µM | [45] |
| $Cu^{2+}$-ISM/PEDOT:PSS/GCE | $Cu^{2+}$ | Potentiometry | 0.5 nM | $28.1 \pm 0.4$ mV $dec^{-1}$ | 1 nM–1 mM | [46] |
| ISMs/PEDOT:PSS/GCE | $Na^+$ | Potentiometry | - | $56 \pm 1$ mV $dec^{-1}$ | 0.1–100 µM | [47] |
| | $K^+$ | | - | $58 \pm 1$ mV $dec^{-1}$ | 0.01 mM–100 µM | |
| | $Ca^{2+}$ | | - | $29 \pm 1$ mV $dec^{-1}$ | 0.01–100 µM | |
| | $Mg^{2+}$ | | - | $30 \pm 1$ mV $dec^{-1}$ | 1–100 µM | |
| | $Cl^-$ | | - | $-54 \pm 1$ mV $dec^{-1}$ | 0.1–100 µM | |
| $Pb^{2+}$-ISM/PEDOT:PSS/GCE | $Pb^{2+}$ | Potentiometry | 0.1 µM | 27 mV $dec^{-1}$ | $10^{-5}$–$10^{-7}$ M | [49] |
| PEDOT:PSS/glassy-carbon disk | thiols | Amperometry | 0.005 mM | 0.43 A $M^{-1}$ $cm^{-2}$ | 0.005–0.1 mM | [50] |
| PEDOT:PSS/GCE | Tricresyl phosphate | Voltammetry | 70 ppb | - | 50–300 ppb | [51] |
| PEDOT:PSS-GO/PET | carbofuran | Voltammetry | 0.1 µM | - | 1 mM–90 mM | [52] |
| PEDOT:PSS-β-CD-SWCNT-COOH/GCE | shikonin | Voltammetry | 1.80 nM | - | 6.0–30,000 nM | [53] |
| PEDOT:PSS-rGO/GCE | nimesulide / piroxicam | Voltammetry | 2.4 nM / 0.1 µM | - | 80–1900 nM / 0.87–260 µM | [54] |
| PEDOT:PSS-G/SPCE | 2,2-diphenyl1-picrylhydrazyl (DPPH) | Amperometry | 0.59 µM | - | 5–30 µM | [55] |
| PEDOT:PSS-MgO/GCE | bisphenol A | Voltammetry | 0.5 nM | - | 1.0 nM–0.4 µM and 0.4–10 µM | [56] |
| CuNPs/GO-CB-PEDOT:PSS/GCE | isoproterenol | Voltammetry | 1.9 µM | 0.062 µA $µM^{-1}$ | 8–50 µM | [57] |
| | acetaminophen | | 0.23 µM | 0.29 µA $µM^{-1}$ | 0.9–7 µM | |
| | folic acid | | 1.0 µM | 0.098 µA $µM^{-1}$ | 5–31 µM | |
| | propranolol | | 0.18 µM | 0.92 µA $µM^{-1}$ | 0.5–2.9 µM | |
| | caffeine | | 3.4 µM | 0.028 µA $µM^{-1}$ | 11–64 µM | |
| PEDOT:PSS-ZnO/GCE | chlorogenic acid | Voltammetry | 0.02 µM | 26.38 µA $mM^{-1}$ $cm^{-2}$ | 0.03–476.2 µM | [58] |
| AgNPs/PEDOT:PSS-$H_2SO_4$/glass | nitrite | Amperometry | 0.34 µM | 0.03639 µA $µM^{-1}$ $cm^{-2}$ | 0.5–3400 µM | [59] |
| PEDOT:PSS-DMSO film | tert-butylhydroquinone | Voltammetry | 0.15 µM | - | 0.5–200 µM | [60] |
| PEDOT:PSS-CMC/GCE | tryptophan | Voltammetry | 0.02 µM | - | 0.05–100 mM | [61] |
| PEDOT:PSS-CMC-SWCNT/GCE | maleic hydrazide | Voltammetry | 0.1 µM | - | 0.8–51 µM | [62] |

## 3. PEDOT:PSS-Based Electronic Chemosensors

Compared with electrochemical chemosensors, electronic chemosensors are relatively simple in construction. Most of them are based on a simple interdigital (IDT) electrode or conductive sensing materials deposited directly on substrates that are connected to a measurement system (Figure 6a,b). The changes in the current, resistance or capacitance [63] caused by the surface interaction with the analytes can be measured and transduced to an output signal. Due to their low cost, small size, and ease of use, electronic chemosensors are commonly used for monitoring humidity and various gases and chemicals.
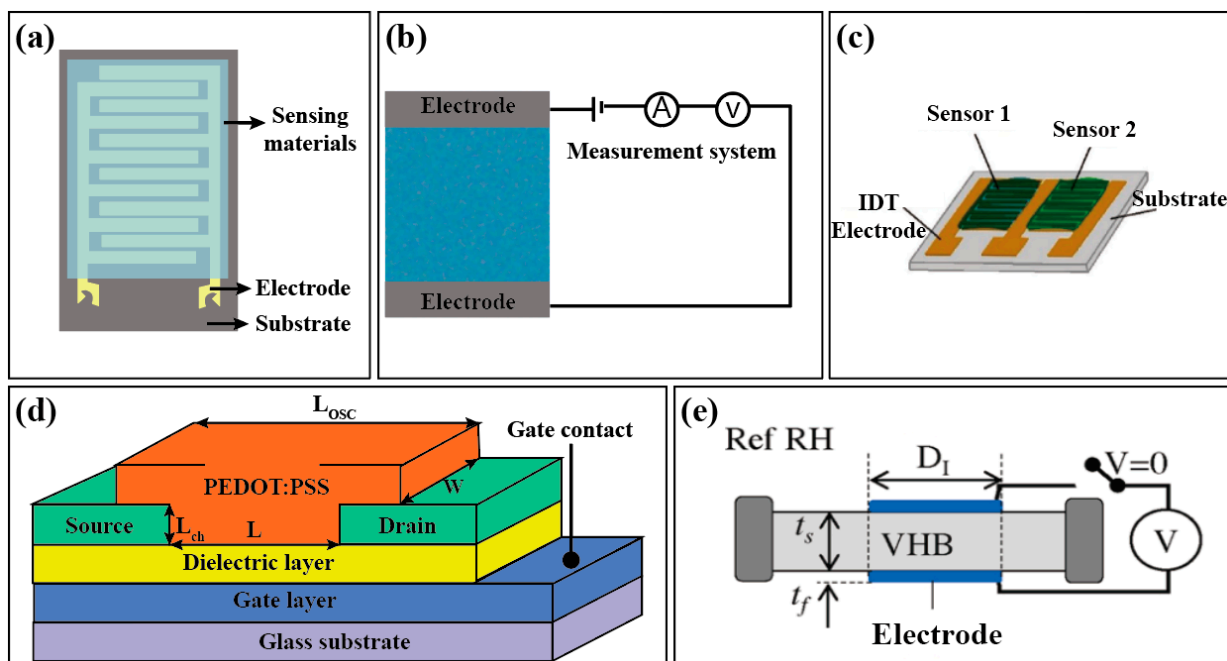


**Figure 6.** Schematic architectures of electronic chemosensors based on PEDOT:PSS and its composites as sensing materials: (**a**) Simple IDT; (**b**) Electrode-based sensors; (**c**) multiple IDTs in series [64]; (**d**) Organic field effect transistor (OFET); (**e**) Dielectric elastomer actuator [65].

In most cases, PEDOT:PSS is deposited on IDT electrodes or other substrates by drop-casting or spin-coating. The resulted pristine PEDOT:PSS film presents a low sensitivity and a slow response because the film's morphology, microstructure and porosity do not satisfy the need of gas sensing performance. Hence, nanostructure engineering of PEDOT:PSS would be crucial for enhancing the gas sensing performance. Typical ways to fabricate nanostructured PEDOT:PSS include nano-confined strategies such as electrospinning [66] and other template methods [67,68]. Furthermore, PEDOT:PSS is printable [10], thus allowing to produce highly uniform films on various flexible substrates such as polyethylene terephthalate (PET) and paper, for which the thickness of the film can be precisely controlled by techniques like inkjet printing.

PEDOT:PSS can also be blended with other functional materials such as carbon materials and metal oxide semiconductors through solution processing, and the composites thus obtained can then be deposited on a substrate through the methods mentioned above to improve the performance of electronic chemosensors. The material composition, structure, sensing mechanism and performance of various PEDOT:PSS composites as used in electronic chemosensors towards humidity, ammonia, $CO_X$, $NO_2$, and volatile organic compounds (VOCs), are listed in Table 2 and discussed accordingly in the following sections.

### 3.1. Humidity Detection

Humidity sensors are widely used in environmental monitoring, healthcare and the construction of electronic and optical devices [10]. It is essential to monitor, detect and

control the ambient humidity in many manufacturing situations. Although numerous studies have been made towards developing humidity sensors, the current research and development in this field still faces many technical challenges regarding both material design and structure engineering.

As a ready-to-use waterborne dispersion, PEDOT:PSS is by nature a water-absorbing material, which remains as a typical problem for its practical application in organic electronic devices (wherein humidity effect or moisture-induced degradation of electronic performance must be avoided). However, such a "negative" effect for electronics can be turned into something positive to enable the development of humidity sensors. PEDOT:PSS films are characterized by a granular structure in which PEDOT-rich grains (conductive) are surrounded by PSS (insulating, hydrophilic). When the relative humidity (RH) increases, a decrease in conductivity of PEDOT:PSS can usually be observed, which is ascribed to the decreasing electrical interconnections among PEDOT chains caused by the water absorption (swelling) of PSS. Humidity sensors based on a PEDOT:PSS film generally demonstrate a linear response towards relative humidity changing from 20% to 80%. However, such PEDOT:PSS materials would lose their sensing function when the humidity exceeds 80% since the conductivity turns to an increase at a RH >80%, which is due to the saturation of the PEDOT:PSS film with water or a water layer formed on the surface of the film (enabling or enhancing ionic conductivity) [69].

In recent years, the humidity sensors based on PEDOT:PSS are mainly fabricated by spin-coating, spray-coating, or drop-casting. These methods have a few disadvantages, such as film inhomogeneity, an uncontrollable shape and a low production efficiency. The non-porous structure produced therefrom also results in a long sensing response and recovery time [70], which limits the application of these sensors in the areas such as respiratory monitoring, wherein the response/recovery cycling must be faster (shorter) than a single respiratory period (normally in 3–4 s) [67]. In addition, the three fabrication methods mentioned above are generally suitable for large-area manufacturing of macroscopic devices, but not microscale miniaturized devices, which are otherwise crucial for integration with other functional devices [71]. In this regard, new efforts have been made in order to develop alternative methods for film fabrication, with the aim of improving sensor performance.

Thanks to the excellent solution processability of PEDOT:PSS, many other methods have been exploited and developed to fabricate films from the polymer composite. Among them, the dipping method [72] was used to blend PEDOT:PSS with nanofiber fabrics, which was suited for development as a humidity sensor. The surface area and open porosity of nanofiber fabrics help improve the sensing performance through enhanced surface absorption of gas analytes. Inkjet printing technology can also be perfectly compatible with PEDOT:PSS, and the material thus printed is usually suited for exploitation as a gas sensor device. The recent advancement in inkjet printing equipment further renders the film fabrication of PEDOT:PSS regarding morphology uniformness and repeatability, low cost, and adaptability to a wide range of substrates and materials [10,73]. This helps facilitate the research and development of PEDOT:PSS composites as electronic chemosensors.

In Wang's recent work [71], a micron line humidity sensor (Figure 7a) was fabricated by printing PEDOT:PSS with a femtosecond laser, for which the laser beam was applied directly to PEDOT:PSS in the channel between two electrodes, thus processing the sample into a designed pattern. This micro-fabrication technology combines the advantages of high precision, arbitrary patterning and a wide selection of processing materials. The dimensional size of the sensor device fabricated was about 6 mm$^2$ and the effective working area was less than 100 μm$^2$. The small size is convenient for integration with other functionalized sensing chips. The sensor exhibited quite a short response/recovery time (0.86 s/0.59 s) (Figure 7e), enabling real-time respiration monitoring of human and rats under different physiological conditions (Figure 7f). Accompanied by human exhalation, the sensor channel is highly moisturized, causing an increased humidity exposure towards the sensor surface. During inhalation, the inhaling air from the atmosphere will reduce the level of humidity around the sensor. The humidity sensor was placed on the skin under the

nose of the tester as shown in Figure 7b. The current versus time curve during respiration is shown in Figure 7c,d, indicating that the PEDOT:PSS micron line humidity sensor can effectively monitor the real-time respiratory rate of human motion.
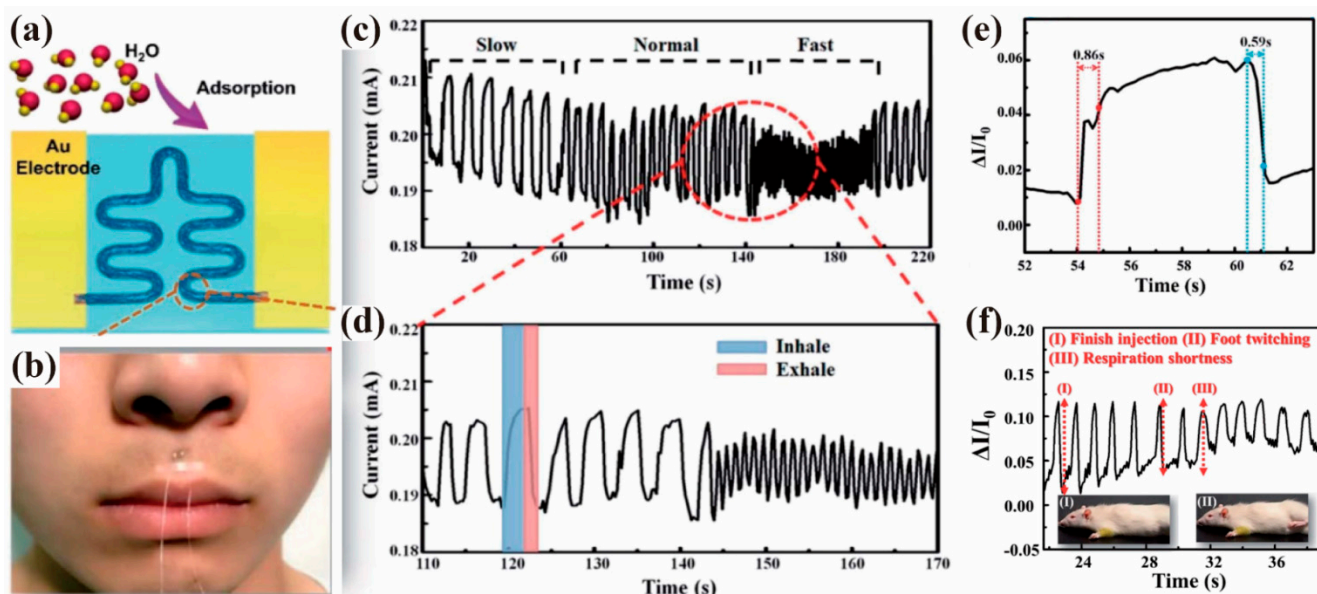


**Figure 7.** (**a**) Working scheme of the PEDOT:PSS micron line humidity sensor; (**b**) photograph of the PEDOT:PSS micron line humidity sensor put on the skin under nose; (**c**) responses of the sensor at different respiratory rate; (**d**) zoom-in view of (**c**) curve in the linear coordinate system; (**e**) the response and recovery curve after switching 69% RH to the ambient atmosphere (RH was approximately 42%); (**f**) respiratory monitoring curves of anesthetized rat before and after injection of nikethamide [71].

Similarly, Duan et al. [67] improved the sensing performance by limiting the dimension of the sensing layer. As shown in Figure 8a, they designed a PDMS (polydimethylsiloxane) mold with nanogrooves (70 nm in width and 80 nm in depth) and placed it in contact with the PET substrate to form nanochannels. Then PEDOT:PSS aqueous solution was cast into the channels. After the solvent completely evaporated, the PDMS mold was removed from the PET substrate, leaving the solidified PEDOT:PSS in the format of nanowires on the PET substrate (Figure 8b). This nano-confined strategy facilitates the absorption/desorption of water molecules and maximizes the sensor response to moisture (Figure 8c), in contrast to the slow adsorption, diffusion, and desorption as observed in the typical network of polymer films (Figure 8d). The nanoscale humidity sensor showed a high sensitivity (5.46%) and ultrafast response (0.63 s) when changing humidity between 0% and 13%. It also demonstrated real-time monitoring of human respiration (Figure 8e) and excellent mechanical durability and robustness (Figure 8f).

PET, PI (Polyimide) and other substrates perform well in flexibility and possess good adhesion to human skin, which greatly facilitates their application in sensors that can potentially be used in electronic skin, and other biomedical and wearable devices. Similarly, paper also possesses good flexibility, while the material cost is extremely low. In this regard, research effort has been made to develop paper-based humidity sensors by blending with PEDOT:PSS [70,74]. Paper has a strong water-absorption rate, making it easy to blend with PEDOT:PSS simply by dipping the paper in an aqueous dispersion of the polymer. The composite thus fabricated takes the intrinsic porous morphology of paper, highly conducive to diffusion and surface absorption of gas analytes, which is in turn desirable for use as a humidity sensor. These flexible substrates are also perfectly integrated with printing technology, showing good flexibility in several types of flexibility tests, including outer/inner bending, twisting, and stretching. These tests show great promise for applications in various emerging flexible electronics and optoelectronic devices.
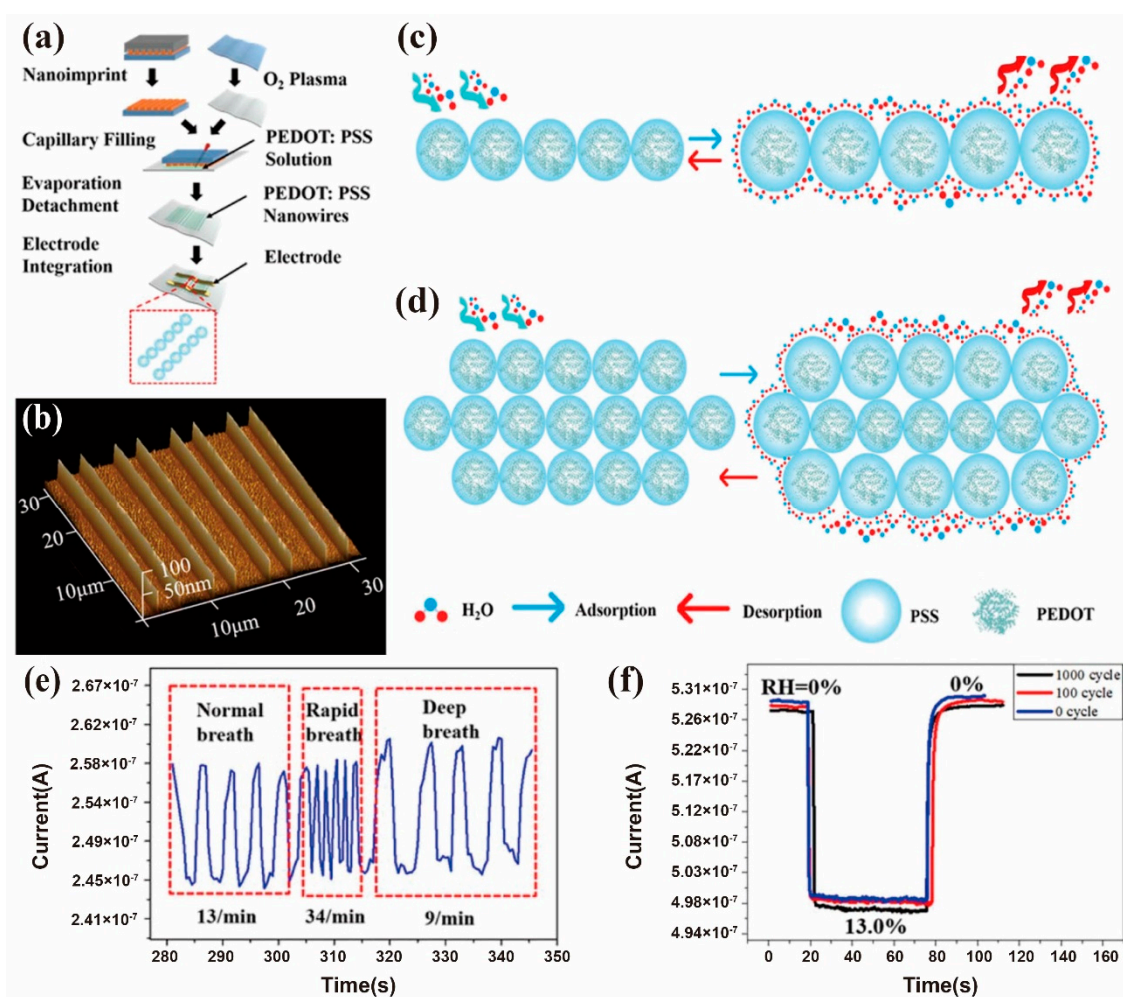
**Figure 8.** (**a**) The fabrication process of PEDOT:PSS nanowire sensors; (**b**) optical microscopy image of the PEDOT:PSS nanowires; schematic of water adsorption and desorption on (**c**) PEDOT:PSS nanowires and (**d**) PEDOT:PSS film; (**e**) the response of the humidity sensor to normal, rapid, and deep respiration; (**f**) response of the humidity sensor under RH switching between 0% and 13% with multiple bending cycles at an outer bending radius of 10 mm [67].

Some technical challenges, such as slow response and recovery, still remain for PEDOT:PSS-based humidity sensors. In order to solve these challenges, piezoelectric LiNbO$_3$ substrate was used to produce surface acoustic waves (SAW), which helped release the water molecules from the sensing layer when the IDT was supplied with a high frequency. As evidenced in Aziz's work [75,76], as shown in Table 2, SAW could indeed significantly improve the recovery time of the PEDOT:PSS humidity sensor.

In addition, PEDOT:PSS has often been combined with other materials, e.g., polyvinyl alcohol (PVA) [76], ZnSnO$_3$ [75], or Fe$_3$O$_4$/$\gamma$-Fe$_2$O$_3$ [69] nanoparticles, to produce a polymer composite in porous structure (Figure 9), which is conducive to the adsorption and desorption of water vapor, and is thus suited for development as a humidity sensor. These PEDOT:PSS composites are expected to further improve the sensing performance, as well as enable some special features or functions intrinsic to the nanoparticles encapsulated. For example, by incorporating the Fe$_3$O$_4$/$\gamma$-Fe$_2$O$_3$ nanoparticles into PEDOT:PSS, the nanostructured films became magnetic, meaning that the film could be easily transferred, simply by using a magnet, onto rigid substrates such as silicon, steel and glass, as well as flexible substrates such as elastomers, paper, plastic frames, or metal weaves in arbitrary shapes and topographies without being damaged or broken [69]. The advantage of using ZnSnO$_3$ nanoparticles as an additive is the wide sensing range (0–90% RH) and the high repeatability (response remains as high as 77% of the initial value after 2 months of continuous operation). Due to the high hydrophilicity of GO, the PEDOT:PSS composite

with GO demonstrated a sensitive chemoresistive and dielectric response towards water vapor, making it an ideal candidate as a humidity sensor. Romero et al. [77] reported on a humidity sensor using PEDOT:PSS-GO composite as the capacitive sensing layer, which showed a sensitivity of 1.22 nF/%RH at 1 kHz.
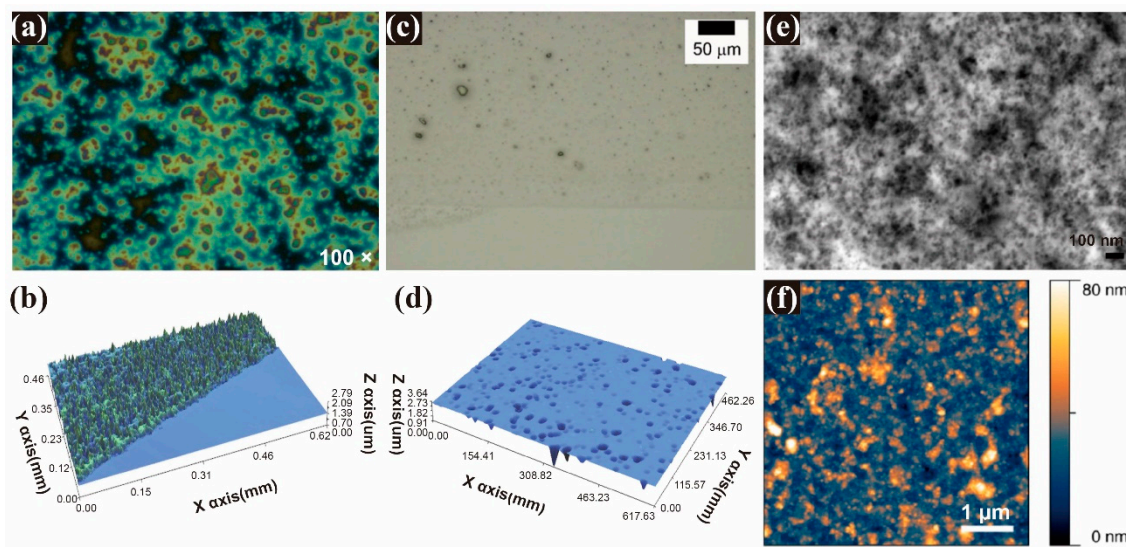


**Figure 9.** (**a**) Microscopy image at $100\times$ resolution and (**b**) surface profile of the sensing layer (PEDOT:PSS-PVA) [76]; (**c**) microscopy image and (**d**) surface profile of the sensing layer (PEDOT:PSS-ZnSnO$_3$) [75]; (**e**) STEM micrograph and (**f**) atomic force microscopy scan of the sensing layer (PEDOT:PSS-Fe$_3$O$_4$/$\gamma$-Fe$_2$O$_3$) [69].

Considering the fact that a humidity sensor with a single active material has a limit in the detection range, some researchers [64,78] chose multiple IDTs fabricated with different active sensor materials connected in a series on a single chip (Figure 6c). For example, GO, PEDOT:PSS, and Methyl Red materials have sensing responses of 0 to 78% RH, 30 to 75% RH, and 25 to 100% RH, respectively. A humidity sensor [78] incorporating all the three sensors on IDT electrodes in a series can detect a full range of humidity from 0% RH to 100% RH with the response and recovery times to be as fast as 1 s and 3.5 s, respectively. Similarly, by connecting the PEDOT:PSS-based portion with the MoS$_2$-based portion in a series, the humidity sensing device [64] showed high sensitivity (50 k$\Omega$/%RH or 800 Hz/%RH) in a wide range of 0% RH–80% RH. In contrast, if the composite film of PEDOT:PSS and MoS$_2$ was fabricated as a humidity sensor, interesting phenomena would occur, i.e., an increase in MoS$_2$ addition would turn the positive resistance response to negative response upon exposure to humidity [79]. This is likely due to the fact that hole carriers generated in MoS$_2$ nanosheets may be injected into the PEDOT:PSS chains absorbed with water molecules, which in turn results in enhanced electrical transport along the PEDOT:PSS chains.

In addition to the chemoresistive sensor (with the sensing materials bridged between two electrodes), PEDOT:PSS has also been fabricated as an organic field effect transistor (OFET) sensor (Figure 6d), which provides additional signal amplification through the gate modulation. Zafar et al. [80] reported on an OFET sensor for detecting humidity, for which PEDOT:PSS film was used as the active channel layer and n-type silicon as the gate electrode. The source–drain current flow is not only controlled by the gate voltage, but is also modulated by humidity level in the ambient environment. Within the humidity range (40–80% RH) examined, the channel current has been observed to amplify by nearly 29.4 times of its magnitude at a drain source voltage of $-40$ V and the gate source voltage of $-10$ V.

Recently, a hydromorphic dielectric elastomer actuator [65] was proposed for high humidity sensing. The device consists of a relatively water-inert acrylic dielectric elastomer layer sandwiched by a pair of hygroscopic PEDOT:PSS electrodes (Figure 6e). The electrodes became softer upon absorption of moisture, allowing for moisture permeation into

the dielectric elastomer substrate during electrical activation and readout. The dielectric elastomeric actuation (under constant voltage) was found to increase with increasing humidity, the current leaking through it rising more significantly. This dielectric elastomer actuator-based humidity sensor remained in working order when a mist of water droplets was sprayed on its electrodes.

### 3.2. Ammonia Detection

Ammonia ($NH_3$) is a colorless and highly toxic gas that is mostly produced from industry, but also exists naturally in the atmosphere at low-ppb to sub-ppb levels. It has been widely used in various applications such as fertilizers, refrigeration, water purification, and manufacturing for nitrogenous products. At high concentrations, $NH_3$ can cause irritation to the skin, eyes, nose, throat, and respiratory tract due to its corrosive properties. Exposure to a massive concentration of $NH_3$ (>5000 ppm) may be fatal within minutes. Therefore, detection of $NH_3$ has attracted a great deal of attention of environment protection and human health [20,81].

When the PEDOT:PSS film is exposed to $NH_3$, the lone pair of electrons of the $NH_3$ molecule interact with the holes of the p-type PEDOT:PSS grains, and such a neutralization interaction leads to a decrease in charge carrier density of the PEDOT domains, which in turn results in a decrease in the conductivity. However, the pristine PEDOT:PSS film exhibits a poor senor response to $NH_3$ because the PEDOT domains are surrounded by PSS, for which the electrical conductivity of the film is largely determined by the resistive PSS regions, outweighing the conductivity change of the PEDOT domains [82]. Furthermore, the presence of water (moisture) in ambient air also increases the electrical resistance of the sensor based on PEDOT:PSS, causing additional interreference to the sensor signal [12]. Particularly at a high level of humidity, more moisture would react with $NH_3$ to produce $NH_4OH$, which leads to a great fluctuation of resistance change between the introduction of $NH_3$ and discharge of the $NH_3$ process [82]. Therefore, the influence of moisture must be taken into account in the design of $NH_3$ sensors. Some critical parameters for evaluation of $NH_3$ sensors were listed in Table 2. The stability of sensors also remains crucial for precise, repeated measurements of $NH_3$ and other gases, especially under trace concentration levels. For example, the baseline resistance of pristine PEDOT:PSS film in one study was found to increase from 3.6 k$\Omega$ to 4.1 k$\Omega$ after five cycles of testing [82]. Such a baseline shift represents one of the common technical challenges for chemosensors that limits their practical applications.

Electronic chemosensors based on a PEDOT:PSS film generally exhibit low sensitivity in response to $NH_3$, mainly due to the limited surface area and nonporous structure. Aiming to enhance the sensing sensitivity, PEDOT:PSS in various nanostructures, including nanowires [68] and nanofibers [66], have been fabricated by either a complex nano-confined strategy, or high voltage electro-spinning. These nanostructured materials demonstrate significant enhancement in sensitivity compared to the pristine films. For example, Duan et al. [68] prepared PEDOT:PSS nanowires using a PDMS mold patterned with nanogrooves, and in comparison with the PEDOT:PSS thin film sensors, these nanowires showed a significantly higher sensitivity and a faster response to $NH_3$, as shown in Figure 10. The increased sensor response was largely attributed to their high surface-volume ratio. These observations indicate that appropriate structural engineering of sensor materials at the nanoscale could enhance the sensor performance, especially the response sensitivity for detection of a low gas concentration.

As mentioned above, the inkjet printing technique has been proven to be effective for fabricating thin films and nanostructures of polyremes like PEDOT:PSS, particularly on flexible substrates like plastic. Inkjet printing is simple, low-cost and capable of large area fabrication with high uniformity, which, combined, make it an ideal technique to prepare flexible gas sensors from PEDOT:PSS films [83]. Moreover, PEDOT:PSS can also be printed together with other functional materials (e.g., graphene [84], $FeCl_3$ [82]) through appropriate solution processing. Inkjet printing has now become one of the most popular

fabrication methods for making flexible gas sensors, taking the advantages of precise control of film thickness and uniformness as deposited. The technical maturation of such a fabrication method will likely promote the research and development of flexible electronics in general, way beyond the chemosensor fields.
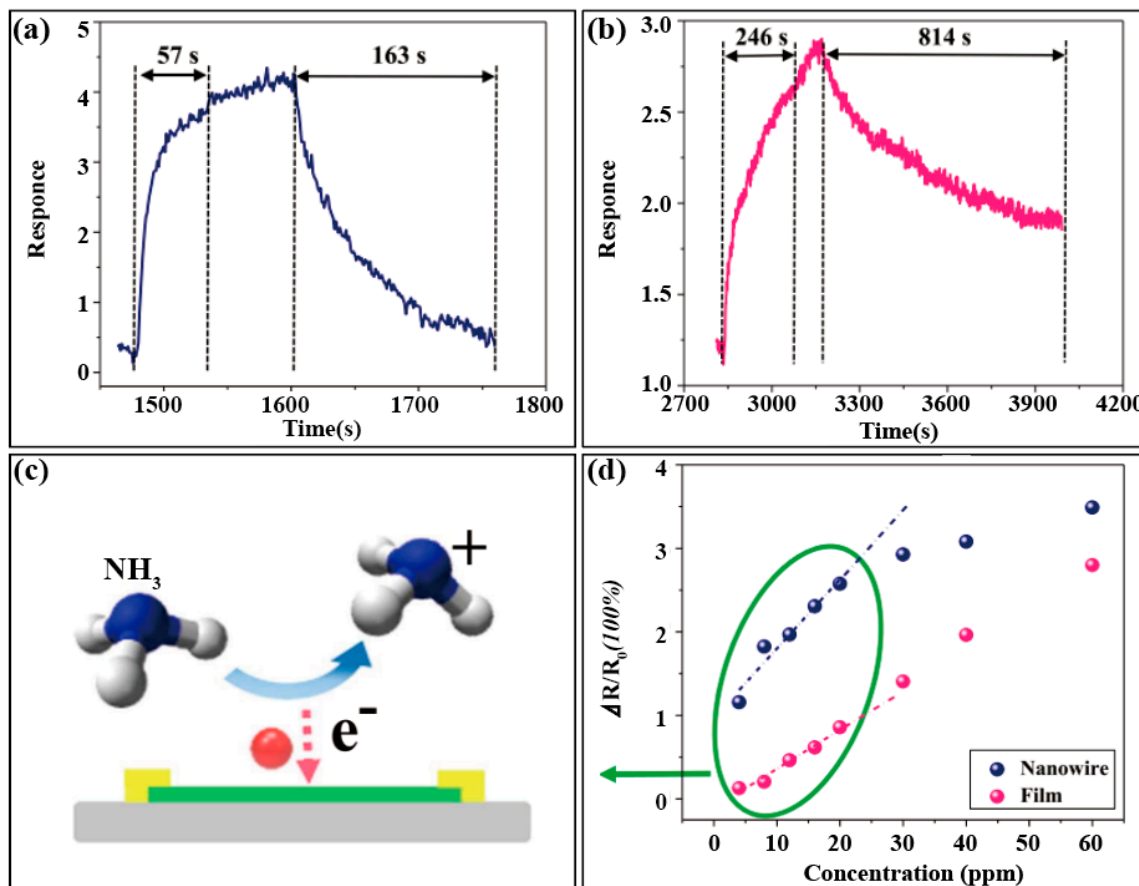


**Figure 10.** Time course of sensor response and recovery obtained for the PEDOT:PSS nanowires (**a**) and thin film (**b**) upon exposure to 60 ppm of $NH_3$; (**c**) Schematic illustration of the chemoresistive sensing mechanism of $NH_3$ gas; (**d**) comparison of the chemoresistive sensing response between PEDOT:PSS nanowires and thin-film upon exposure to $NH_3$ under varying concentrations [68].

Currently, the main drawback of pristine PEDOT:PSS film used in $NH_3$ sensors lies in its low conductivity and gas sensitivity. This technical problem can be overcome by blending PEDOT:PSS with other electroactive nanomaterials, such as MWCNTs [83], graphene [12,84,85], reduced graphene oxide (rGO) [86] and silver nanowires (AgNWs) [20,87]. These nanomaterials can be mixed homogeneously with the polymer matrix, producing maximal interfacial contact and helping improve the sensing performance. The doped nanomaterials were found to be capable of enhancing significantly the conductivity of PEDOT:PSS, as well as the sensing performance in comparison to the pristine polymer. Guo et al. [20,87] fabricated PEDOT:PSS composite films doped with AgNWs by spin-coating successively a AgNWs dispersion and PEDOT:PSS aqueous solution on PET substrate and tested the chemoresistive sensing for $NH_3$. The surface bumps at the interface regions induced by the embedded AgNWs under the PEDOT:PSS film can enhance the absorption of $NH_3$ molecules and thus increase the interface resistance between AgNWs and PEDOT:PSS, which leads to a significant enhancement of detection sensitivity towards $NH_3$. Inclusion of graphene or rGO in PEDOT:PSS was also found to be able to increase the conductivity depending on the doping concentration and mesoscopic interfacial structure of the blending. The incorporation of graphene in PEDOT:PSS led to a considerable enhancement of the $NH_3$

response, which was ascribed to a combination of several factors such as an increase in the specific surface area, intrinsic sensing properties of graphene, and π-π interaction between graphene and PEDOT:PSS (helping facilitating the charge transfer) [12]. By doping rGO into PEDOT:PSS [86], a large number of charge carriers (both polarons and bi-polarons) can be generated in the polymer matrix. These charge carriers can be easily transported through the polymer chain, helping improve the chemoresistive sensor response of the PEDOT:PSS film. Moreover, the doping with rGO would also improve the surface roughness and the high surface/volume ratio of PEDOT:PSS film, which are both crucial for enhancing the gas absorption and electrical interaction with the polymer matrix [85].

### 3.3. CO and $CO_2$ Detection

For CO or $CO_2$ sensors, PEDOT:PSS is often used as a host and guest material in hybrid systems due to its good electrical conductivity, film-forming properties and solution processability. The gas sensitivity and selectivity of PEDOT:PSS to CO [88,89] can be improved by blending PEDOT:PSS with metal complexes that have a strong binding towards CO. For example, PEDOT:PSS films doped with 0.1wt. % Co(salen) or Fe(salen) complexes demonstrated a high chemoresistive sensor response towards CO (a flow rate of 19.0 mL min$^{-1}$ and 8 mL s$^{-1}$, respectively.), $-25.0 \pm 0.05\%$ and $-31.32 \pm 0.88\%$, respectively. A new pyrimidine-fused heterocyclic compound, bis(2hydroxyphenyl)dihydropyrido [2,3-d:6,5-d]dipyrimidine-tetraone (B2HDDT), was also employed as a molecular dopant for PEDOT:PSS by Memarzadeh et al. [90] B2HDDT contains numerous functional groups that can form hydrogen bonds with CO and PEDOT:PSS, thus helping capture CO within the polymer matrix and improve the detection sensitivity. In Kim's recent work [91], a porous PEDOT:PSS-MWCNTs composite was exploited for CO sensing. Although the surface coating of PEDOT:PSS reduced the number of adsorption sites on CNT, the conductive polymer layer thus coated helps bridge the CNTs electrically and form a network with high conductivity, which facilitates the long range charge transport and ultimately leads to enhancement in gas sensing.

The graphene layer and the PEDOT:PSS layer were printed on PET layer by layer to manufacture the $CO_2$ sensor [92]. The variation of the electrical conductivity of graphene due to gas molecule adsorption and the conductivity of the graphene layer increases when the concentration of the $CO_2$ gas increases. The main reason to use a layer of PEDOT:PSS under the sensing layer of graphene is to realize a uniform layer over IDT electrodes, guaranteeing continuity of the resistive contact between IDT fingers and a layer with a resistance value higher than the pure IDT electrode. This allows for making dominant the effect of the resistance variation of the graphene layer, super-imposed to the PEDOT:PSS layer. Considering the effect of exogenous factors such as humidity on the PEDOT:PSS layer, graphene as the outer layer can also performed as a shield.

The existence of moisture is critical for $CO_2$ detection. Chuang et al. [93] developed a $CO_2$ sensing material based on PEDOT:PSS blended with PANI. The effects of humidity on PEDOT:PSS and PANI counteract each other in the conductivity change characteristic. As $CO_2$ and $H_2O$ molecular adsorption increased, the conductivity of PEDOT:PSS-PANI increased because of the carbonate formation between $CO_2$ and the secondary amine backbone of PANI. This resulted in a high selectivity between $CO_2$ and $H_2O$ molecules of the developed PEDOT:PSS-PANI sensing composite.

### 3.4. $NO_2$ Detection

$NO_2$ is a toxic air pollutant mainly released in the automotive industry and vehicles. It greatly threatens environmental security due to its role as a source of photochemical smog and acid rain. Therefore, it is demanding to develop inexpensive, sensitive, selective and simple devices to detect low concentrations of $NO_2$ gas at room temperature ambient conditions for environmental monitoring [94]. $NO_2$ is a strong electron withdrawing molecule that can easily deplete electrons from the sensing material, causing changes in the conductivity. PEDOT:PSS composites mixed with semiconducting metal oxides

(e.g., $WO_3$ [94,95], $TiO_2$ [96]) have been proven to be effective for detection of $NO_2$, even at room temperature. Metal oxide semiconductors have been commonly used as chemoresistive materials for sensing redox active gases or chemical analytes through interfacial charge transfer interaction. However, the metal oxides normally suffer from the high operation temperature (typically 200 to 500 °C). The new approach with PEDOT:PSS composites may provide an alternative way to solve this technical challenge for metal oxide sensors.

Blending PEDOT:PSS with metal oxide semiconductors (especially in the format of nanoparticles) provides dual functions. On the one hand, PEDOT:PSS provides conducting channels for the charge carriers, thereby producing a much lower initial resistance, helping enhance the signal-to-noise ratio for the sensing response. On the other hand, the heterojunctions formed at the interface between metal oxide and PEDOT:PSS would provide abundant adsorption sites for gas analytes, thus maximizing the chemoresistive sensing response. Indeed, a chemoresistive sensor based on PEDOT:PSS-$WO_3$ composite exhibited a low initial resistance (~870 Ω) and a good sensing response (~1.2) towards 50 ppb $NO_2$ gas at room temperature, with a response and recovery time of 45.1 and 88.7 s, respectively [95].

### 3.5. Volatile Organic Compounds (VOCs) Detection

The increased emission of harmful VOCs, such as methanol [97–100], acetone [101], formaldehyde [102], and nitrobenzene [103], has been widely considered as a serious threat to the environment and to human health, as these toxic VOCs are proven to be correlated with the increasing cases of many diseases [99], such as allergies, asthma, cancer, and emphysema. Therefore, it is essential to monitor the concentration of VOCs in the environment in real time.

Many VOCs are chemically or electrically active, meaning that they are capable of inducing a change in the conductivity of the PEDOT:PSS, thus generating a chemoresistive signal response. Various substrates such as PDMS, PET, paper, even cotton [101] have been used for the construction of PEDOT:PSS sensors for gas phase detection of VOCs. Fabrication of PEDOT:PSS films on a substrate can be realized with various processing methods, including drop-casting [100], dipping method [101], inkjet printing [102], etc. More interesting, Sarkar et al. [99] adopted a novel fabrication approach by firstly creating quasi-periodic cracks in PEDOT:PSS film using strain, followed by engineering the crack morphology with controlled plasma etching (Figure 11). These engineered cracks provide electrical conduction pathways that can be turned on and off in response to absorption of methanol vapor, which enables ultra-high sensitivity for chemoresistive sensing with an on/off ratio as high as $10^6$. A variety of nanomaterials have been blended with PEDOT:PSS to fabricate composites suited for chemoresistive sensing of VOCs, as listed in Table 2. Most of these composites possess a large surface area that is conducive to absorption of gas analytes, resulting in a high sensor performance.

Wang et al. [100] fabricated a methanol gas sensor by blending PEDOT:PSS with $Ti_3C_2T_x$ at a mass ratio of 4:1. As one of the most widely studied two-dimensional transition metal carbides (MXene), $Ti_3C_2T_x$ has been proven to be a promising gas-sensing material that can be used to detect ultralow concentration of gases at room temperature. The high sensing sensitivity of $Ti_3C_2T_x$ is due to the large specific surface area and the plenty of surface functional groups that endow $Ti_3C_2T_x$ with abundant active sites for interacting with gas molecules. When tested at room temperature, the PEDOT:PSS-$Ti_3C_2T_x$ composite possessed a high response ratio of the largest response and the second largest response (5.54) and an enhanced response compared to pure PEDOT:PSS and pure $Ti_3C_2T_x$ for methanol gas. The high sensing response was due to the increased interlayer spacing between PEDOT:PSS and $Ti_3C_2T_x$ (allowing for increased absorption of gas analytes) while still maintaining a high conductivity.

**Table 2.** Comparison of PEDOT:PSS-based electrical chemosensors for different analytes.

| Sensing Material | Mechanism | Sensor Structure | Analyte | Sensitivity | Response/Recovery Time | Sensing Range | Reference |
|---|---|---|---|---|---|---|---|
| PEDOT:PSS | Capacitance | IDT | Humidity | - | <30 s/<1 min | 52.0–93.4% RH | [63] |
| PEDOT:PSS/MoS$_2$ | Impedance | Dual IDT's in series Sensor array | Humidity | 50 kΩ/%RH, 850 Hz/%RH | 0.5 s/0.8 s | 0–80% RH | [64] |
| PEDOT:PSS | Resistance | Dielectric elastomer actuator | Humidity | - | - | 30–90%RH | [65] |
| PEDOT:PSS | Resistance | Nanowires | Humidity | 5.46% | 0.63 s/2.05 s | 0–60% RH | [67] |
| PEDOT:PSS-Fe$_3$O$_4$/γ-Fe$_2$O$_3$ | Resistance | electrodes on substrate | Humidity | 0.65%/ΔRH | >1 s/>1 s | 30–70%RH | [69] |
| PEDOT:PSS-Graphene | Resistance | paper substrate | Humidity | - | - | 20–90% RH | [70] |
| PEDOT:PSS | Resistance | micron line | Humidity | 0.19% (ΔR/R0)/%RH | 0.86 s/0.59 s | 11–69% RH | [71] |
| PEDOT:PSS)/polyacrylonitrile fabrics | Resistance | IDT | Humidity | 110% | 2 s/7 s | 0–100% RH | [72] |
| PEDOT:PSS-ZnSnO$_3$ | Impedance | IDT with SAW effect | Humidity | - | 0.2 s/0.2 s | 0–90%RH | [75] |
| PEDOT:PSS–PVA | Impedance Capacitance | IDT with SAW effect | Humidity | 350 Ω/%RH 28 pF/%RH | 0.63 s/0.56 s | 0–80% RH | [76] |
| PEDOT:PSS/GO | Capacitance | Two interdigitally arranged IDT | Humidity | 1.22 nF/%RH | - | 25–85% RH | [77] |
| PEDOT:PSS-MoS$_2$ | Impedance based | Glass substrates | Humidity | - | - | 50–75% RH | [79] |
| PEDOT:PSS-Graphene | Resistance | IDT | NH$_3$ | 116.38% (1000 ppm) | 7.7 min/10 min | −1500 ppm | [12] |
| AgNWs/PEDOT:PSS | Resistance | PET substrate | NH$_3$ | 5% (1 ppm) | - | 0.5–25 ppm | [20] |
| PEDOT:PSS nanowire | Resistance | Silicon substrate | NH$_3$ | 0.8% (3.2 ppm) | 57 s/163 s | 3–60 ppm | [66] |
| Si/PEDOT:PSS ITO/PEDOT:PSS | Current | OFET | NH$_3$ NH$_3$ | - - | 13 s/8 s 29 s/22 s | - | [81] |
| PEDOT:PSS-FeCl$_3$ | Resistance | IDT | NH$_3$ | 7.6% (0.5 ppm) | 20 s | 0.1–200 ppm | [82] |
| PEDOT:PSS-MWCNTs | Resistance | IDT | NH$_3$ | 73.7% (1000 ppm) | - | 0–1000 ppm | [83] |
| PEDOT:PSS-graphene | Resistance | IDT | NH$_3$ | 6.9% (1000 ppm) | 3 min/5 min | 25–1000 ppm | [84] |
| (CuTSPc@3D-(N)GF)/(PEDOT-PSS) | Resistance | IDT | NH$_3$ | - | - | 1–1000 ppm | [85] |
| PEDOT-PSS rGO | Resistance | IDT | NH$_3$ | - | 1.05 min/2.84 min | - | [86] |
| PEDOT:PSS-Co(salen) | Resistance | IDT | CO | 25.0 ± 0.05% | - | 0.5–10.0% CO (*v/v*) N$_2$ | [88] |
| PEDOT:PSS-Fe(III)(salen) | Resistance | IDT | CO | 31.32 ± 0.88% | 38 s/5 s | - | [89] |
| PEDOT:PSS-B2HDDT | Resistance | PET substrate | CO | 55% (common gas) | - | 0–66 vol% | [90] |
| PEDOT:PSS-MWCNTs | Resistance | PDMS substrate | CO | 0.05 ± 0.004% (1000 ppm) | 10.6 ± 0.4 s/24.6 ± 1.2 s | 250–1000 ppm | [91] |
| Graphene/PEDOT:PSS | Resistance | PET substrate | CO$_2$ | 4.7 μΩ/Ω/ppm (420 ppm) | - | 400–4200 ppm | [92] |
| PEDOT:PSS-PANI | Resistance | IDT | CO | 3.24% (1000 ppm) | - | 500–2000 ppm | [93] |
| PEDOT:PSS-WO$_3$ | Resistance | IDT | NO$_2$ | 2.31 (80 ppm) | - | 10–80 ppm | [94] |
| PEDOT:PSS-WO$_3$ | Resistance | IDT | NO$_2$ | - | 45.1 s/88.7 s | 50–220 ppb | [95] |
| PEDOT:PSS-TiO$_2$ | Current | IDT | NO$_2$ | - | - | 10–130 ppb | [96] |
| PEDOT:PSS-graphene | Resistance | IDT | Methanol | 13.5% (50 ppm) | 12 s/32 s | 1–1000 ppm | [97] |
| PEDOT:PSS-GO | Resistance | IDT | Methanol | 11% (35 ppm) | 3.2 s/16 s | 3–700 ppm | [98] |
| PEDOT:PSS thin film | Resistance | PDMS substrate | Methanol | ~$10^6$ (300 ppm) | <5 s/<5 s | 6–300 ppm | [99] |
| PEDOT:PSS-Ti$_3$C$_2$Tx | Resistance | IDT | Methanol | 5.54 | - | - | [100] |
| PEDOT:PSS-cotton | Current | Cotton | Acetone | 53% | 1 min/2 min | 1–30% (acetone solvent) | [101] |
| PEDOT:PSS-MWCNTs | Resistance | IDT | Formaldehyde | 30.5% (10 ppm) | 45 s/<7 s | 10–200 ppm | [102] |
| PEDOT:PSS-graphite nanosheets | Resistance | Glass substrate | Nitroaromatics | - | 1.15 min/1.88 min | - | [103] |
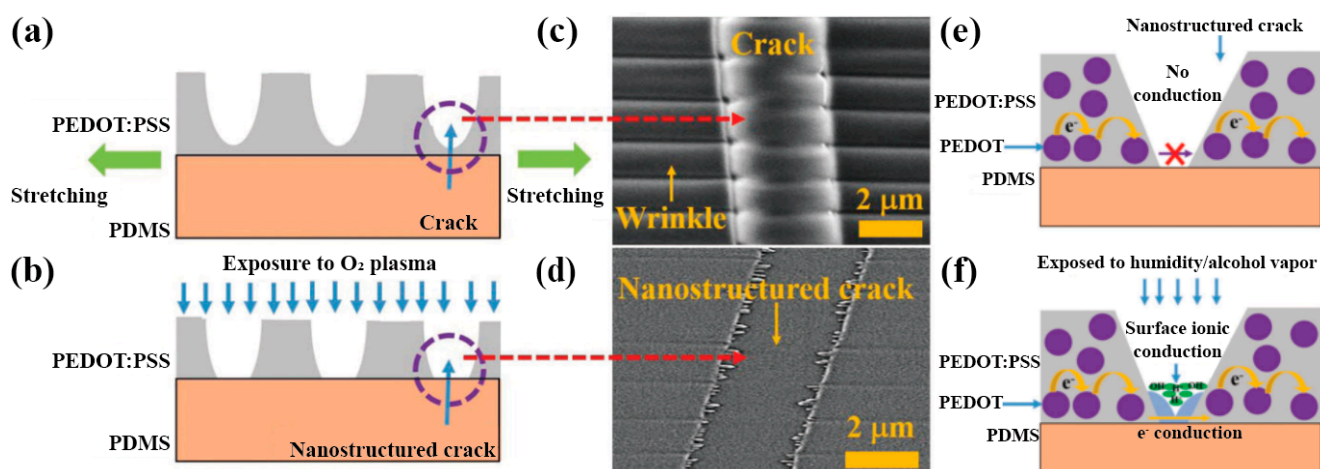
**Figure 11.** Cross-section schematic diagrams of the uniaxially strained film (**a**) and nanostructured crack morphology of a stretched PEDOT:PSS thin film (**b**) after $O_2$ plasma etching; SEM images of the surface morphology of a 20% strained PEDOT:PSS thin film (**c**) and a PEDOT:PSS thin film with nanostructured cracks (**d**); Cross-section schematic diagrams of nanostructured PEDOT:PSS thin film (**e**) and its exposure to high humidity/alcohol vapors (**f**). The tapering of the crack near the substrate is shown by the blue region. The yellow arrow indicates the electron percolation pathway [99].

The combination of PEDOT:PSS with other carbon nanomaterials (graphene [97], GO [98], MWCNTs [102], etc.) represents another potential solution to enhance the sensitivity and selectivity of the chemoresistive sensing for VOCs. The incorporation of these carbon materials into PEDOT:PSS resulted in a significant increase in charge carrier concentration. For example, the conductivity of a pristine PEDOT:PSS film and the composite blended with N-doped graphene quantum dots, were measured to be 650 and 1365 S cm$^{-1}$, respectively, using a 4-point probe technique under an applied current of 10 nA [97]. Moreover, the high density of chemical groups (especially hydroxyl and carboxylic groups) on GO can also enhance the surface adsorption of VOCs through hydrogen bonding along with other chemical interactions, which in turn may lead to much improved detection sensitivity towards VOCs [98].

## 4. Conclusions and Perspective

In conclusion, significant achievements have been achieved in PEDOT:PSS and its composites as applied in electrochemical and electronic chemosensors over the past decade, for which a wealth of novel materials, design principles, and sensing mechanisms have been developed. Most of the research advancements relied on the design and optimization of PEDOT:PSS composites, in correlation with the specific film and nanostructure fabrication techniques that are suited for production of a sensor device in large scale and with sufficient reproducibility. In this regard, the emerging nanomaterials (e.g., those based on carbons, metal oxides, etc.) and nanoscale engineering methods and instrumentation have now commonly been employed to help the fabrication of PEDOT:PSS composites and film printing on various substrates, including the flexible ones that are ideal for manufacturing wearable devices.

Although PEDOT:PSS has many advantages such as an adjustable electrical conductivity, mechanical flexibility, strong solution processability and good biocompatibility, there are still some technical concerns that need to be solved or improved before the PEDOT:PSS-based sensors can be practically used, especially in the fields of flexible or wearable electronics. For electrochemical sensors, PEDOT:PSS or its composites with other nanomaterials are often coated onto a substrate to function as a working electrode. One of the existing problems with such electrodes is that the PEDOT:PSS coating may swell or even fall off the electrode when immersed in aqueous solution. Although some research efforts

(e.g., covered with a Nafion film) have been made to improve the robustness of PEDOT:PSS coating, the extra coverage layer like Nafion would likely inhibit the contact between PEDOT:PSS and analytes. The same water-swelling problem may also be encountered in electronic sensors employing PEDOT:PSS film as the active material. When operated in an ambient atmosphere with a high humidity, the absorption and condensation of moisture on the film could cause degradation of the electrical conductivity or sensing performance. Solutions to this water-related stability problem are expected to rely on the design of a new material structure, for which appropriate additives may be blended homogeneously with the polymer to enhance the hydrophobicity (thus minimizing the water absorption) while still maintaining the high electrical conductivity and solution processability intrinsic to PEDOT:PSS.

As a typical polymer that is suited for development as flexible or wearable electronics, even with self-healing characteristics, PEDOT:PSS-based chemosensors have been extensively exploited with the aim to be adapted with flexible substrate or integrated with wearable systems. Specific research efforts have also been made to shrink the size of the sensors so as to be suited for integration with other electronic devices like data transmission and communication. However, traditional film fabrication methods and the associated structure engineering techniques are not suited for the construction of small devices or system miniaturization. In this regard, the emerging nanofiber and cleanroom technologies (e.g., nanopatterning, nano-lithography, nano-templating, etc.) will provide great potential for the fabrication of nanostructured films or devices, which in turn would facilitate the system integration and miniaturization. With the versatile coating and structural engineering techniques, PEDOT:PSS or its composites can be modified onto other flexible substrates with a diverse shape and mechanical properties, such as cotton fiber, paper, PET, etc., which are not only flexible, stretchable or bendable, but moreover have a low cost and are environmentally benign, thus serving as ideal candidates for use in future wearable electronics. Moreover, the tensile, mechanical strength and electrical conductivity of PEDOT:PSS films can be adjusted by adding solvents such as DMSO, EG, etc. [104]. This provides more options to modulate and optimize the electrical and mechanical properties of PEDOT:PSS in order to match the technical needs of different types of sensors.

**Author Contributions:** S.C. and L.Z. proposed the review topic and its outline, wrote and revised the manuscript. N.G. organized and wrote the manuscript. J.Y., Q.T., J.S. and M.Z. helped in improving the manuscript regarding format, language, Figures and Tables. All authors discussed and commented on the manuscript. All authors have read and agreed to the published version of the manuscript.

**Conflicts of Interest:** The authors declare no conflict of interest.

# References

1. Kumar, H.; Kumari, N.; Sharma, R. Nanocomposites (conducting polymer and nanoparticles) based electrochemical biosensor for the detection of environment pollutant: Its issues and challenges. *Environ. Impact Assess. Rev.* **2020**, *85*, 106438. [CrossRef]
2. Nezakati, T.; Seifalian, A.; Tan, A.; Seifalian, A.M. Conductive polymers: Opportunities and challenges in biomedical applications. *Chem. Rev.* **2018**, *118*, 6766–6843. [CrossRef]
3. Ramdzan, N.S.M.; Fen, Y.W.; Anas, N.A.A.; Omar, N.A.S.; Saleviter, S. Development of biopolymer and conducting polymer-based optical sensors for heavy metal ion detection. *Molecules* **2020**, *25*, 2548–2573. [CrossRef] [PubMed]
4. Wen, Y.P.; Xu, J.K. Scientific importance of water-processable PEDOT-PSS and preparation, challenge and new application in sensors of its film electrode: A review. *J. Polym. Sci. Part A Polym. Chem.* **2017**, *55*, 1121–1150. [CrossRef]
5. Dubey, N.; Kushwaha, C.S.; Shukla, S.K. A review on electrically conducting polymer bionanocomposites for biomedical and other applications. *Int. J. Polym. Mater. Polym. Biomater.* **2019**, *69*, 709–727. [CrossRef]
6. Zamiri, G.; Haseeb, A. Recent trends and developments in graphene/conducting polymer nanocomposites chemiresistive sensors. *Materials* **2020**, *13*, 3311. [CrossRef] [PubMed]

7. Bae, J.; Hwang, Y.; Park, S.-H.; Park, S.J.; Lee, J.; Kim, H.J.; Jang, A.; Park, S.; Kwon, O.S. An elaborate sensor system based on conducting polymer-oligosaccharides in hydrogel and the formation of inclusion complexes. *J. Ind. Eng. Chem.* **2020**, *90*, 266–273. [CrossRef]

8. Mantione, D.; Del Agua, I.; Sanchez-Sanchez, A.; Mecerreyes, D. Poly(3,4-ethylenedioxythiophene) (PEDOT) derivatives: Innovative conductive polymers for bioelectronics. *Polymers* **2017**, *9*, 354. [CrossRef]

9. Cho, K.H.; Yu, H.; Lee, J.S.; Jang, J. Facile synthesis of palladium-decorated three-dimensional conducting polymer nanofilm for highly sensitive H$_2$ gas sensor. *J. Mater. Sci.* **2020**, *55*, 5156–5165. [CrossRef]

10. Morais, R.M.; Klem, M.d.S.; Nogueira, G.L.; Gomes, T.C.; Alves, N. Low cost humidity sensor based on PANI/PEDOT:PSS printed on paper. *IEEE Sens. J.* **2018**, *18*, 2647–2651. [CrossRef]

11. Tajik, S.; Beitollahi, H.; Nejad, F.G.; Shoaie, I.S.; Khalilzadeh, M.A.; Asl, M.S.; Van Le, Q.; Zhang, K.; Jang, H.W.; Shokouhimehr, M. Recent developments in conducting polymers: Applications for electrochemistry. *RSC Adv.* **2020**, *10*, 37834–37856. [CrossRef]

12. Hakimi, M.; Salehi, A.; Boroumand, F.A. Fabrication and characterization of an ammonia gas sensor based on PEDOT-PSS with n-doped graphene quantum dots dopant. *IEEE Sens. J.* **2016**, *16*, 6149–6154. [CrossRef]

13. Rahimzadeh, Z.; Naghib, S.M.; Zare, Y.; Rhee, K.Y. An overview on the synthesis and recent applications of conducting poly(3,4-ethylenedioxythiophene) (PEDOT) in industry and biomedicine. *J. Mater. Sci.* **2020**, *55*, 7575–7611. [CrossRef]

14. Elschner, A.; Kirchmeyer, S.; Lövenich, W.; Merker, U.; Reuter, K. *PEDOT-Principles and Applications of an Intrinsically Conductive Polymer*; CRC Press: New York, NY, USA, 2011.

15. Zheng, Y.; Zeng, H.N.; Zhu, Q.; Xu, J.W. Recent advances in conducting poly(3,4-ethylenedioxythiophene):polystyrene sulfonate hybrids for thermoelectric applications. *J. Mater. Chem. C* **2018**, *6*, 8858–8873. [CrossRef]

16. Sun, K.; Zhang, S.P.; Li, P.C.; Xia, Y.J.; Zhang, X.; Du, D.H.; Isikgor, F.H.; Ouyang, J.Y. Review on application of PEDOTs and PEDOT:PSS in energy conversion and storage devices. *J Mater. Sci. Mater Electron.* **2015**, *26*, 4438–4462. [CrossRef]

17. Ouyang, J.Y. Recent advances of intrinsically conductive polymers. *Acta Phys. Chim. Sin.* **2018**, *34*, 1211–1220. [CrossRef]

18. Kaur, G.; Kaur, A.; Kaur, H. Review on nanomaterials/conducting polymer based nanocomposites for the development of biosensors and electrochemical sensors. *Polym. Plast. Tech. Mat.* **2020**, *60*, 502–519. [CrossRef]

19. Chen, Y.C.; O'Hare, D. Exhaled breath condensate based breath analyser-a disposable hydrogen peroxide sensor and smart analyser. *Analyst* **2020**, *145*, 3549–3556. [CrossRef]

20. Li, S.Y.; Chen, S.J.; Zhuo, B.G.; Li, Q.F.; Liu, W.J.; Guo, X.J. Flexible ammonia sensor based on PEDOT:PSS/silver nanowire composite film for meat freshness monitoring. *IEEE Electr. Device L.* **2017**, *38*, 975–978. [CrossRef]

21. Kayser, L.V.; Lipomi, D.J. Stretchable Conductive polymers and composites based on PEDOT and PEDOT: PSS. *Adv. Mater.* **2019**, *31*, 1806133. [CrossRef]

22. Reynolds, J.R.; Tompson, B.C.; Skotheim, T.A. *Conjugated Polymers: Properties, Processing, and Applications*; CRC Press: New York, NY, USA, 2019.

23. Liao, J.J.; Si, H.W.; Zhang, X.D.; Lin, S.W. Functional sensing interfaces of PEDOT: PSS organic electrochemical transistors for chemical and biological sensors: A mini review. *Sensors* **2019**, *19*, 218–233. [CrossRef]

24. Yan, Y.J.; Wu, X.M.; Chen, Q.Z.; Liu, Y.Q.; Chen, H.P.; Guo, T.L. High-performance low-voltage flexible photodetector arrays based on all-solid-state organic electrochemical transistors for photosensing and imaging. *ACS Appl. Mater. Inter.* **2019**, *11*, 20214–20224. [CrossRef] [PubMed]

25. Choosang, J.; Thavarungkul, P.; Kanatharana, P.; Numnuam, A. AuNPs/PpPD/PEDOT: PSS-Fc modified screen-printed carbon electrode label-free immunosensor for sensitive and selective determination of human serum albumin. *Microchem. J.* **2020**, *155*, 104709–104716. [CrossRef]

26. Abd-Wahab, F.; Abdul Guthoos, H.F.; Wan Salim, W.W.A. Solid-state rGO-PEDOT: PSS transducing material for cost-effective enzymatic sensing. *Biosensors* **2019**, *9*, 36–50. [CrossRef] [PubMed]

27. Bhasin, A.; Sanders, E.C.; Ziegler, J.M.; Briggs, J.S.; Drago, N.P.; Attar, A.M.; Santos, A.M.; True, M.Y.; Ogata, A.F.; Yoon, D.V.; et al. Virus bioresistor (VBR) for detection of bladder cancer marker DJ-1 in urine at 10 pM in one minute. *Anal. Chem.* **2020**, *92*, 6654–6666. [CrossRef]

28. El-Said, W.A.; Abdelshakour, M.; Choi, J.H.; Choi, J.W. Application of conducting polymer nanostructures to electrochemical biosensors. *Molecules* **2020**, *25*, 307–317. [CrossRef]

29. Amirzadeh, Z.; Javadpour, S.; Shariat, M.H.; Knibbe, R. Non-enzymatic glucose sensor based on copper oxide and multi-wall carbon nanotubes using PEDOT: PSS matrix. *Synth. Met.* **2018**, *245*, 160–166. [CrossRef]

30. Mariani, F.; Gualandi, I.; Tonelli, D.; Decataldo, F.; Possanzini, L.; Fraboni, B.; Scavetta, E. Design of an electrochemically gated organic semiconductor for pH sensing. *Electrochem. Commun.* **2020**, *116*, 106763–106770. [CrossRef]

31. Khodagholy, D.; Rivnay, J.; Sessolo, M.; Gurfinkel, M.; Leleux, P.; Jimison, L.H.; Stavrinidou, E.; Herve, T.; Sanaur, S.; Owens, R.M. High transconductance organic electrochemical transistors. *Nat. Commun.* **2013**, *4*, 2133. [CrossRef]

32. Borras-Brull, M.; Blondeau, P.; Riu, J. The use of conducting polymers for enhanced electrochemical determination of hydrogen peroxide. *Crit. Rev. Anal. Chem.* **2020**, 1–14. [CrossRef]

33. Zhang, R.L.; Xu, X.F.; Fan, X.X.; Yang, R.C.; Wu, T.; Zhang, C.G. Application of conducting micelles self-assembled from commercial poly(3,4-ethylenedioxythiophene):poly(styrene sulfonate) and chitosan for electrochemical biosensor. *Colloid Polym. Sci.* **2018**, *296*, 495–502. [CrossRef]

34. Słoniewska, A.; Kasztelan, M.; Berbeć, S.; Pałys, B. Influence of buffer solution on structure and electrochemical properties of poly(3,4-ethylenedioxythiophene)/poly(styrenesulfonate) hydrogels. *Synth. Met.* **2020**, *263*, 116363–116369. [CrossRef]

35. Xu, J.J.; Peng, R.; Ran, Q.; Xian, Y.Z.; Tian, Y.; Jin, L.T. A highly soluble poly(3,4-ethylenedioxythiophene)-poly(styrene sulfonic acid)/Au nanocomposite for horseradish peroxidase immobilization and biosensing. *Talanta* **2010**, *82*, 1511–1515. [CrossRef] [PubMed]

36. Yao, Y.Y.; Wen, Y.P.; Zhang, L.; Xu, J.K.; Wang, Z.F.; Duan, X.M. A stable sandwich-type hydrogen peroxide sensor based on immobilizing horseradish peroxidase to a silver nanoparticle monolayer supported by PEDOT: PSS-nafion composite electrode. *Int. J. Electrochem. Sci.* **2013**, *8*, 9348–9359.

37. Mercante, L.A.; Facure, M.H.M.; Sanfelice, R.C.; Migliorini, F.L.; Mattoso, L.H.C.; Correa, D.S. One-pot preparation of PEDOT: PSS-reduced graphene decorated with Au nanoparticles for enzymatic electrochemical sensing of $H_2O_2$. *Appl. Surf. Sci.* **2017**, *407*, 162–170. [CrossRef]

38. Siao, H.-W.; Chen, S.-M.; Lin, K.-C. Electrochemical study of PEDOT-PSS-MDB-modified electrode and its electrocatalytic sensing of hydrogen peroxide. *J. Solid State Electr.* **2010**, *15*, 1121–1128. [CrossRef]

39. Zahed, M.A.; Barman, S.C.; Das, P.S.; Sharifuzzaman, M.; Yoon, H.S.; Yoon, S.H.; Park, J.Y. Highly flexible and conductive poly (3, 4-ethylene dioxythiophene)-poly (styrene sulfonate) anchored 3-dimensional porous graphene network-based electrochemical biosensor for glucose and pH detection in human perspiration. *Biosens. Bioelectron.* **2020**, *160*, 112220–112229. [CrossRef]

40. Smith, R.E.; Totti, S.; Velliou, E.; Campagnolo, P.; Hingley-Wilson, S.M.; Ward, N.I.; Varcoe, J.R.; Crean, C. Development of a novel highly conductive and flexible cotton yarn for wearable pH sensor technology. *Sens. Actuator B Chem.* **2019**, *287*, 338–345. [CrossRef]

41. Naficy, S.; Oveissi, F.; Patrick, B.; Schindeler, A.; Dehghani, F. Printed, flexible pH sensor hydrogels for wet environments. *Adv. Mater. Technol. US* **2018**, *3*, 1800137–1800146. [CrossRef]

42. Shi, H.; Liu, C.C.; Jiang, Q.L.; Xu, J.K. Effective approaches to improve the electrical conductivity of PEDOT:PSS: A review. *Adv. Electron. Mater.* **2015**, *1*, 1500017–1500032. [CrossRef]

43. Reid, D.O.; Smith, R.E.; Garcia-Torres, J.; Watts, J.F.; Crean, C. Solvent treatment of wet-spun PEDOT:PSS fibers for fiber-based wearable pH sensing. *Sensors* **2019**, *19*, 4213–4222. [CrossRef] [PubMed]

44. Coppedè, N.; Giannetto, M.; Villani, M.; Lucchini, V.; Battista, E.; Careri, M.; Zappettini, A. Ion selective textile organic electrochemical transistor for wearable sweat monitoring. *Org. Electron.* **2020**, *78*, 105579–105584. [CrossRef]

45. Keene, S.T.; Fogarty, D.; Cooke, R.; Casadevall, C.D.; Salleo, A.; Parlak, O. Wearable organic electrochemical transistor patch for multiplexed sensing of calcium and ammonium ions from human perspiration. *Adv. Healthc. Mater.* **2019**, *8*, 1901321–1901328. [CrossRef] [PubMed]

46. Abd, E.A.; Mohamed, A.-O.; Ayman, H.K.; Elsayed, A.E. Single-piece solid contact Cu(2+)-selective electrodes based on a synthesized macrocyclic calix[4]arene derivative as a neutral carrier ionophore. *Molecules* **2019**, *24*, 920–931.

47. Urbanowicz, M.; Pijanowska, D.G.; Jasiński, A.; Ekman, M.; Bocheńska, M.K. A miniaturized solid-contact potentiometric multisensor platform for determination of ionic profiles in human saliva. *J. Solid State Electr.* **2019**, *23*, 3299–3308. [CrossRef]

48. Ocana, C.; Munoz-Correas, M.; Abramova, N.; Bratov, A. Comparison of different commercial conducting materials as ion-to-electron transducer layers in low-cost selective solid-contact electrodes. *Sensors* **2020**, *20*, 1348–1359. [CrossRef] [PubMed]

49. Wagner, M.; Lisak, G.; Ivaska, A.; Bobacka, J. Durable PEDOT: PSS films obtained from modified water-based inks for electrochemical sensors. *Sens. Actuator B Chem.* **2013**, *181*, 694–701. [CrossRef]

50. Shadrina, A.A.; Nikiforova, T.G.; Poturai, D.O. Fabrication of electrodes modified with poly-3,4-ethylenedioxythiophene-polystyrene sulfonate film and study of their applicability in thiol-sensitive sensors. *Russ. J. Appl. Chem.* **2015**, *88*, 423–429. [CrossRef]

51. Yang, X.; Kirsch, J.; Olsen, E.V.; Fergus, J.W.; Simonian, A.L. Anti-fouling PEDOT: PSS modification on glassy carbon electrodes for continuous monitoring of tricresyl phosphate. *Sens. Actuator B Chem.* **2013**, *177*, 659–667. [CrossRef]

52. Chekol, F.; Mehretie, S.; Hailu, F.A.; Tolcha, T.; Megersa, N.; Admassie, S. Roll-to-roll printed PEDOT/PSS/GO plastic film for electrochemical determination of carbofuran. *Electroanalysis* **2019**, *31*, 1104–1111. [CrossRef]

53. Chai, J.D.; Zhang, J.; Wen, Y.P.; Zou, L.; Zhang, X.X.; Xin, X.; Zhou, M.H.; Xu, J.K.; Zhang, G. Highly sensitive electrochemical sensor based on PEDOT:PSS-β-CD-SWCNT-COOH modified glassy carbon electrode enables trace analysis shikonin. *J. Electrochem. Soc.* **2019**, *166*, B388–B394. [CrossRef]

54. Wong, A.; Santos, A.M.; Fatibello-Filho, O. Determination of piroxicam and nimesulide using an electrochemical sensor based on reduced graphene oxide and PEDOT: PSS. *J. Electroanal. Chem.* **2017**, *799*, 547–555. [CrossRef]

55. Tirawattanakoson, R.; Rattanarat, P.; Ngamrojanavanich, N.; Rodthongkum, N.; Chailapakul, O. Free radical scavenger screening of total antioxidant capacity in herb and beverage using graphene/PEDOT:PSS-modified electrochemical sensor. *J. Electroanal. Chem.* **2016**, *767*, 68–75. [CrossRef]

56. Zheng, L. An electrochemical sensor on the novel MgO-PEDOT: PSS platform for sensitive bisphenol a determination. *Int. J. Electrochem. Sc.* **2019**, *14*, 9030–9041. [CrossRef]

57. Wong, A.; Santos, A.M.; Silva, T.A.; Fatibello-Filho, O. Simultaneous determination of isoproterenol, acetaminophen, folic acid, propranolol and caffeine using a sensor platform based on carbon black, graphene oxide, copper nanoparticles and PEDOT:PSS. *Talanta* **2018**, *183*, 329–338. [CrossRef]

58. Manivannan, K.; Sivakumar, M.; Cheng, C.-C.; Lu, C.-H.; Chen, J.-K. An effective electrochemical detection of chlorogenic acid in real samples: Flower-like ZnO surface covered on PEDOT: PSS composites modified glassy carbon electrode. *Sensor. Actuat. B-Chem.* **2019**, *301*, 127002–127009. [CrossRef]

59. Pang, D.; Ma, C.; Chen, D.Z.; Shen, Y.L.; Zhu, W.Q.; Gao, J.J.; Song, H.O.; Zhang, X.M.; Zhang, S.P. Silver nanoparticle-functionalized poly (3, 4-ethylenedioxythiophene): Polystyrene film on glass substrate for electrochemical determination of nitrite. *Org. Electron.* **2019**, *75*, 105374–105380. [CrossRef]

60. Tian, Q.Y.; Xu, J.K.; Xu, Q.; Duan, X.M.; Jiang, F.X.; Lu, L.M.; Jia, H.Y.; Jia, Y.H.; Li, Y.Y.; Yu, Y.F. A poly(3,4-ethylenedioxythiophene): poly(styrenesulfonate)-based electrochemical sensor for tert.-butylhydroquinone. *Mikrochim. Acta* **2019**, *186*, 772–779. [CrossRef] [PubMed]

61. Zhang, H.; Xu, J.K.; Wen, Y.P.; Wang, Z.F.; Zhang, J.; Ding, W.C. Conducting poly(3,4-ethylenedioxythiophene):poly(styrene-sulfonate) film electrode with superior long-term electrode stability in water and synergistically enhanced electrocatalytic ability for application in electrochemical sensors. *Synth. Met.* **2015**, *204*, 39–47. [CrossRef]

62. Zhang, J.; Xu, J.K.; Wen, Y.P.; Wang, Z.F.; Zhang, H.; Ding, W.C. Voltammetric determination of phytoinhibitor maleic hydrazide using PEDOT:PSS composite electrode. *J. Electroanal. Chem.* **2015**, *751*, 65–74. [CrossRef]

63. Yao, X.S.; Cui, Y. A PEDOT: PSS functionalized capacitive sensor for humidity. *Measurement* **2020**, *160*, 107782. [CrossRef]

64. Siddiqui, G.U.; Sajid, M.; Ali, J.; Kim, S.W.; Doh, Y.H.; Choi, K.H. Wide range highly sensitive relative humidity sensor based on series combination of MoS$_2$ and PEDOT:PSS sensors array. *Sens. Actuator B Chem.* **2018**, *266*, 354–363. [CrossRef]

65. Shrestha, M.; Lu, Z.; Lau, G.-K. High humidity sensing by 'hygromorphic' dielectric elastomer actuator. *Sens. Actuator B Chem.* **2021**, *329*, 129268–129275. [CrossRef]

66. Pinto, N.J.; Rivera, D.; Melendez, A.; Ramos, I.; Lim, J.H.; Johnson, A.T.C. Electrical response of electrospun PEDOT-PSSA nanofibers to organic and inorganic gases. *Sens. Actuator B Chem.* **2011**, *156*, 849–853. [CrossRef]

67. Zhou, C.; Zhang, X.S.; Tang, N.; Fang, Y.; Zhang, H.N.; Duan, X.X. Rapid response flexible humidity sensor for respiration monitoring using nano-confined strategy. *Nanotechnology* **2020**, *31*, 125302–125329. [CrossRef]

68. Tang, N.; Jiang, Y.; Qu, H.M.; Duan, X.X. Conductive polymer nanowire gas sensor fabricated by nanoscale soft lithography. *Nanotechnology* **2017**, *28*, 485301–485326. [CrossRef]

69. Taccola, S.; Greco, F.; Zucca, A.; Innocenti, C.; Fernandez Cde, J.; Campo, G.; Sangregorio, C.; Mazzolai, B.; Mattoli, V. Characterization of free-standing PEDOT:PSS/iron oxide nanoparticle composite thin films and application as conformable humidity sensors. *ACS. Appl. Mater. Inter.* **2013**, *5*, 6324–6332. [CrossRef]

70. Popov, V.I.; Kotin, I.A.; Nebogatikova, N.A.; Smagulova, S.A.; Antonova, I.V. Graphene-PEDOT:PSS humidity sensors for high sensitive, low-cost, highly-reliable, flexible, and printed electronics. *Materials* **2019**, *12*, 3477–3485. [CrossRef] [PubMed]

71. Wang, G.; Zhang, Y.; Yang, H.; Wang, W.; Dai, Y.-Z.; Niu, L.-G.; Lv, C.; Xia, H.; Liu, T. Fast-response humidity sensor based on laser printing for respiration monitoring. *RSC Adv.* **2020**, *10*, 8910–8916. [CrossRef]

72. Panapoy, M.; Singsang, W.; Ksapabutr, B. Electrically conductive poly(3,4-ethylenedioxythiophene)-poly(styrene sulfonate)/polyacrylonitrile fabrics for humidity sensors. *Phys. Scripta* **2010**, *T139*, 014056–014060. [CrossRef]

73. Yuan, Y.; Peng, B.; Chi, H.; Li, C.; Liu, R.; Liu, X.Y. Layer-by-layer inkjet printing SPS:PEDOT NP/RGO composite film for flexible humidity sensors. *RSC Adv.* **2016**, *6*, 113298–113306. [CrossRef]

74. Zhang, Y.L.; Cui, Y. A flexible calligraphy-integrated in situ humidity sensor. *Measurement* **2019**, *147*, 106853–106858. [CrossRef]

75. Aziz, S.; Chang, D.E.; Doh, Y.H.; Kang, C.U.; Choi, K.H. Humidity sensor based on PEDOT: PSS and zinc stannate nano-composite. *J. Electron. Mater.* **2015**, *44*, 3992–3999. [CrossRef]

76. Choi, K.H.; Sajid, M.; Aziz, S.; Yang, B.-S. Wide range high speed relative humidity sensor based on PEDOT: PSS-PVA composite on an IDT printed on piezoelectric substrate. *Sens. Actuat. A-Phys.* **2015**, *228*, 40–49. [CrossRef]

77. Romero, F.J.; Rivadeneyra, A.; Becerer, M.; Morales, D.P.; Rodriguez, N. Fabrication and Characterization of Humidity Sensors Based on Graphene Oxide-PEDOT: PSS Composites on a Flexible Substrate. *Micromachines* **2020**, *11*, 148–162. [CrossRef] [PubMed]

78. Hassan, G.; Sajid, M.; Choi, C. Highly sensitive and full range detectable humidity sensor using PEDOT: PSS, methyl red and graphene oxide materials. *Sci. Rep.* **2019**, *9*, 15227–15236. [CrossRef]

79. Mombrú, D.; Romero, M.; Faccio, R.; Mombrú, A.W. Transition from positive to negative electrical resistance response under humidity conditions for PEDOT:PSS-MoS$_2$ nanocomposite thin films. *J. Mater. Sci.-Mater. El.* **2019**, *30*, 5959–5964. [CrossRef]

80. Zafar, Q.; Abdullah, S.M.; Azmer, M.I.; Najeeb, M.A.; Qadir, K.W.; Sulaiman, K. Influence of relative humidity on the electrical response of PEDOT:PSS based organic field-effect transistor. *Sens. Actuator B Chem.* **2018**, *255*, 2652–2656. [CrossRef]

81. Amer, K.; Elshaer, A.M.; Anas, M.; Ebrahim, S. Fabrication, characterization, and electrical measurements of gas ammonia sensor based on organic field effect transistor. *J. Mater. Sci. Mater. Electron.* **2018**, *30*, 391–400. [CrossRef]

82. Lv, D.W.; Chen, W.G.; Shen, W.F.; Peng, M.Y.; Zhang, X.S.; Wang, R.F.; Xu, L.; Xu, W.; Song, W.J.; Tan, R.Q. Enhanced flexible room temperature ammonia sensor based on PEDOT:PSS thin film with FeCl$_3$ additives prepared by inkjet printing. *Sens. Actuator B Chem.* **2019**, *298*, 126890–126897. [CrossRef]

83. Pakdee, U.; Thaibunnak, A. Growth of MWCNTs on plasma ion-bombarded thin gold films and their enhancements of ammonia-sensing properties using inkjet printing. *J. Nanotechnol.* **2019**, *2019*, 1–11. [CrossRef]

84. Seekaew, Y.; Lokavee, S.; Phokharatkul, D.; Wisitsoraat, A.; Kerdcharoen, T.; Wongchoosuk, C. Low-cost and flexible printed graphene-PEDOT:PSS gas sensor for ammonia detection. *Org. Electron.* **2014**, *15*, 2971–2981. [CrossRef]

85. Dehsari, H.S.; Gavgani, J.N.; Hasani, A.; Mahyari, M.; Shalamzari, E.K.; Salehi, A.; Taromi, F.A. Copper(ii) phthalocyanine supported on a three-dimensional nitrogen-doped graphene/PEDOT-PSS nanocomposite as a highly selective and sensitive sensor for ammonia detection at room temperature. *RSC. Adv.* **2015**, *5*, 79729–79737. [CrossRef]

86. Pasha, A.; Khasim, S.; Khan, F.A.; Dhananjaya, N. Fabrication of gas sensor device using poly (3, 4-ethylenedioxythiophene)-poly (styrenesulfonate)-doped reduced graphene oxide organic thin films for detection of ammonia gas at room temperature. *Iran. Polym. J.* **2019**, *28*, 183–192. [CrossRef]

87. Zhou, H.Y.; Li, S.Y.; Chen, S.J.; Zhang, Q.Q.; Liu, W.J.; Guo, X.J. Enabling low cost flexible smart packaging system with internet-of-things connectivity via flexible hybrid integration of silicon RFID chip and printed polymer sensors. *IEEE Sens. J.* **2020**, *20*, 5004–5011. [CrossRef]

88. Memarzadeh, R.; Panahi, F.; Javadpour, S.; Ali, K.-N.; Noh, H.-B.; Shim, Y.-B. The interaction of CO to the Co(salen) complex in to PEDOT:PSS film and sensor application. *B. Korean Chem. Soc.* **2012**, *33*, 1297–1302. [CrossRef]

89. Arabloo, F.; Javadpour, S.; Memarzadeh, R.; Panahi, F.; Davazdah Emami, M.; Shariat, M.H. The interaction of carbon monoxide to Fe(III)(salen)-PEDOT:PSS composite as a gas sensor. *Synth. Met.* **2015**, *209*, 192–199. [CrossRef]

90. Memarzadeh, R.; Noh, H.-B.; Javadpour, S.; Panahi, F.; Feizpour, A.; Shim, Y.-B. Carbon monoxide sensor based on a $B_2HDDT$-doped PEDOT: PSS layer. *Bull. Korean Chem. Soc.* **2013**, *34*, 2291–2296. [CrossRef]

91. Kim, H.; Jang, Y.; Lee, G.W.; Yang, S.Y.; Jung, J.; Oh, J. Tunable chemical grafting of three-dimensional poly (3, 4-ethylenedioxythiophene)/poly (4-styrenesulfonate)-multiwalled carbon nanotubes composite with faster charge-carrier transport for enhanced gas sensing performance. *Sensors* **2020**, *20*, 2470–2481. [CrossRef]

92. Andò, B.; Baglio, S.; Di Pasquale, G.; Pollicino, A.; Graziani, S.; Gugliuzzo, C.; Lombardo, C.; Marletta, V. Direct printing of a multi-layer sensor on pet substrate for $CO_2$ detection. *Energies* **2019**, *12*, 557–566. [CrossRef]

93. Chuang, W.-Y.; Wu, C.-C.; Su, Y.-C.; Chen, H.-H.; Chiu, H.-W.; Lu, S.-S.; Lin, C.-T. A low-power PEDOT: PSS/EB-PANI for $CO_2$ sensing material integrated with a self-powered sensing platform. *IEEE Sens. J.* **2020**, *20*, 55–61. [CrossRef]

94. Shinde, S.; Jiang, C.-Y.; Zheng, C.-X.; Wang, Y.-Z.; Lin, K.-M.; Koinkar, P.M. Room-temperature and flexible PEDOT: $PSS-WO_3$ gas sensor for nitrogen dioxide detection. *Mod. Phys. Lett. B* **2019**, *33*, 1940013–1940018. [CrossRef]

95. Lin, Y.J.; Huang, L.; Chen, L.; Zhang, J.K.; Shen, L.; Chen, Q.; Shi, W.Z. Fully gravure-printed $NO_2$ gas sensor on a polyimide foil using $WO_3$-PEDOT:PSS nanocomposites and Ag electrodes. *Sens. Actuator B Chem.* **2015**, *216*, 176–183. [CrossRef]

96. Zampetti, E.; Pantalei, S.; Muzyczuk, A.; Bearzotti, A.; De Cesare, F.; Spinella, C.; Macagnano, A. A high sensitive $NO_2$ gas sensor based on PEDOT-$PSS/TiO_2$ nanofibres. *Sens. Actuator B Chem.* **2013**, *176*, 390–398. [CrossRef]

97. Gavgani, J.N.; Dehsari, H.S.; Hasani, A.; Mahyari, M.; Shalamzari, E.K.; Salehi, A.; Taromi, F.A. A room temperature volatile organic compound sensor with enhanced performance, fast response and recovery based on N-doped graphene quantum dots and poly(3,4-ethylenedioxythiophene)-poly(styrenesulfonate) nanocomposite. *RSC Adv.* **2015**, *5*, 57559–57567. [CrossRef]

98. Hasani, A.; Dehsari, H.S.; Gavgani, J.N.; Shalamzari, E.K.; Salehi, A.; Afshar Taromi, F.; Mahyari, M. Sensor for volatile organic compounds using an interdigitated gold electrode modified with a nanocomposite made from poly(3,4-ethylenedioxythiophene)-poly(styrenesulfonate) and ultra-large graphene oxide. *Microchim. Acta* **2015**, *182*, 1551–1559. [CrossRef]

99. Sarkar, B.; Satapathy, D.K.; Jaiswal, M. Nanostructuring mechanical cracks in a flexible conducting polymer thin film for ultra-sensitive vapor sensing. *Nanoscale* **2018**, *11*, 200–210. [CrossRef] [PubMed]

100. Wang, X.F.; Sun, K.M.; Li, K.; Li, X.; Gogotsi, Y. $Ti_3C_2T$/PEDOT: PSS hybrid materials for room-temperature methanol sensor. *Chin. Chem. Lett.* **2020**, *31*, 1018–1021. [CrossRef]

101. Zhang, Y.L.; Cui, Y. Cotton-based wearable PEDOT: PSS electronic sensor for detecting acetone vapor. *Flex. Print. Electron.* **2017**, *2*, 042001–042018. [CrossRef]

102. Timsorn, K.; Wongchoosuk, C. Inkjet printing of room-temperature gas sensors for identification of formalin contamination in squids. *J. Mater. Sci.-Mater. El.* **2019**, *30*, 4782–4791. [CrossRef]

103. Rattan, S.; Singhal, P.; Verma, A.L. Synthesis of PEDOT: PSS (poly(3,4-ethylenedioxythiophene))/poly(4-styrene sulfonate))/ngps (nanographitic platelets) nanocomposites as chemiresistive sensors for detection of nitroaromatics. *Polym. Eng. Sci.* **2013**, *53*, 2045–2052. [CrossRef]

104. Xin, X.; Xue, Z.X.; Gao, N.; Yu, J.R.; Liu, H.T.; Zhang, W.N.; Xu, J.K.; Chen, S. Effects of conductivity-enhancement reagents on self-healing properties of PEDOT:PSS films. *Synth. Met.* **2020**, *268*, 116503–116510. [CrossRef]